

POLITECNICO DI MILANO

Facoltà di Ingegneria Industriale e dell'Informazione

Corso di laurea magistrale in

Chemical Engineering



**Process modelling and simulation of a
methanol synthesis plant using syngas
streams obtained from biomass**

Relatore: Prof. Carlo Giorgio Visconti

Tesi di laurea di:

Domenico Leo Matr. 892765

Anno accademico 2017/2018

Summary

Abbreviation	iv
List of Figures	vi
List of Tables	ix
Nomenclature	xi
Glossary	xiv
Estratto	xvi
Abstract	xviii
Preface	xx
1 Introduction	1
1.1 Theoretical Background.....	5
1.1.1 Biomass gasification	5
1.1.2 Methanol Synthesis.....	6
1.2 State of the art	10
1.2.1 Bio-Syngas Production	10
1.2.2 Methanol Synthesis.....	11
2 Materials and Methods	14
2.1 Setting the environment.....	15
2.2 Process streams.....	16
2.3 Compressors.....	17
2.4 Coolers and Heaters	18
2.5 Mixer and splitter	19
2.6 Reactor.....	20
2.7 Flash.....	21
2.8 Recycle Operator.....	21
2.9 Component Splitter	22
3 Model Building and Validation	25
3.1 Assumption	26
3.2 General Data.....	27
3.3 Reactor section.....	27
3.3.1 Kinetic scheme	29
3.4 Separation and recycle section	30
3.4 Model Validation	31
3.6 Separation section with flash.....	35

4	Different cases simulations	39
4.1	Identification of the new inlet stream	39
4.2	Stream 2E simulation	41
4.2.1	Constant N_T	41
4.2.2	Constant Reactor Inlet / N_T	43
4.2.3	Adding H_2	49
4.2.4	Lurgi Configuration	52
4.3	Stream 2D simulation	58
4.3.1	Constant N_T	58
4.3.2	Constant Reactor Inlet / N_T	59
4.3.3	Adding H_2	61
5	Conclusion	65
	Appendix A	69
	Appendix B	71
	Appendix C	73
	Appendix D	75
	Appendix E	77
	Appendix F	79
	Appendix G	81
	Ringraziamenti	88

Abbreviation

NMD	Normalized Methanol Productivity
RR	Recycle Ratio
RI	Reactor Inlet
RO	Reactor Outlet
FF	Fresh Feed
NG	Natural Gas
PFR	Plug Flow Reactor
BIO	Biological
LHC	Light Hydrocarbons

List of Figures

FIGURE 1.1 TYPES OF RENEWABLE ENERGY [2].	1
FIGURE 1.2 METHANOL PROVENIENCE AND USAGE [3].	3
FIGURE 1.3 METHANOL DEMAND AND PRODUCTION [5].	3
FIGURE 1.4 METHANOL SYNTHESIS LOOP [6].	4
FIGURE 1.5 METHANOL PRODUCTIVITY AND RECYCLE RATIO VS M_F [7].	8
FIGURE 1.6 METHANOL REACTION RATE VS TEMPERATURE [17].	9
FIGURE 1.7 PROFILE OF METHANOL CONVERSION VS TEMPERATURE FOR A QUENCH REACTOR [17].	11
FIGURE 1.8 DESIGN OF A QUENCH REACTOR [15].	12
FIGURE 1.9 DESIGN OF A MULTITUBULAR REACTOR [17].	12
FIGURE 2.1 METHANOL SYNTHESIS LOOP IN ASPEN HYSYS V8.8.	14
FIGURE 2.2 SET OF THE ENVIRONMENT IN ASPEN HYSYS.	15
FIGURE 2.3 LIST OF FLUID PACKAGES.	15
FIGURE 2.4 PROCESS AND ENERGY STREAMS.	16
FIGURE 2.5 PROCESS STREAM WORKSHEET.	16
FIGURE 2.6 THREE PHASES OF A COMPRESSOR.	17
FIGURE 2.7 COMPRESSOR PARAMETERS.	18
FIGURE 2.8 COOLERS AND HEATERS.	19
FIGURE 2.9 MIXER AND SPLITTER.	19
FIGURE 2.10 REACTOR.	20
FIGURE 2.11 REACTION SET ATTACHMENT.	20
FIGURE 2.12 FLASH.	21
FIGURE 2.13 RECYCLE OPERATOR.	22
FIGURE 2.14 COMPONENT SPLITTER.	22
FIGURE 3.1 METHANOL SYNTHESIS LOOP [7].	25
FIGURE 3.2 MOLAR FLOWS INSIDE THE REACTOR.	32
FIGURE 3.3 TEMPERATURE AND PRESSURE PROFILE AT CENTERLINE VS REACTOR LENGTH. BLUE SOLID LINE: TEMPERATURE, RED DASHED LINE: PRESSURE.	34
FIGURE 3.4 TEMPERATURE AND PRESSURE PROFILE FROM MONTEBELLI ET AL. [7].	34
FIGURE 3.5 TEMPERATURE AND PRESSURE PROFILE AT CENTERLINE VS REACTOR LENGTH FOR THE IMPROVED MODEL. BLUE SOLID LINE: TEMPERATURE, RED DASHED LINE: PRESSURE.	36
FIGURE 3.6 MOLAR FLOWS INSIDE THE REACTOR FOR THE IMPROVED MODEL.	37
FIGURE 4.1 TEMPERATURE AND PRESSURE PROFILE AT CENTERLINE VS REACTOR LENGTH FOR STREAM 2E WITH CONSTANT $N_T = 4650$. BLUE SOLID LINE: TEMPERATURE, RED DASHED LINE: PRESSURE.	41
FIGURE 4.2 TEMPERATURE AND PRESSURE PROFILE AT CENTERLINE VS REACTOR LENGTH FOR STREAM 2E WITH CONSTANT $N_T = 4650$ AND FLOW RATIO = 0.9995. BLUE SOLID LINE: TEMPERATURE, RED DASHED LINE: PRESSURE.	42
FIGURE 4.3 TEMPERATURE AND PRESSURE PROFILE AT CENTERLINE VS REACTOR LENGTH FOR STREAM 2E WITH CONSTANT $R_I/N_T = 3.877$ KMOL/H PER EACH TUBE. BLUE SOLID LINE: TEMPERATURE, RED DASHED LINE: PRESSURE.	43
FIGURE 4.4 TEMPERATURE AND PRESSURE PROFILE AT CENTERLINE VS REACTOR LENGTH FOR STREAM 2E WITH CONSTANT $R_I/N_T = 3.877$ KMOL/H PER EACH TUBE AND T_{COOL} DECREASE TO 507.15 K. BLUE SOLID LINE: TEMPERATURE, RED DASHED LINE: PRESSURE.	45

LIST OF FIGURES

FIGURE 4.5 TEMPERATURE AND CO MOLAR FLOW FOR SIMULATION WITH AS FRESH FEED STREAM 2E. BLUE LINE: $T_{\text{cool}} = 507.15$ K AND $T_{\text{in}} = 323$ K; ORANGE LINE: $T_{\text{in}} = T_{\text{cool}} = 508.35$ K; CONTINUE LINE: TEMPERATURE [K]; DASHED LINE: CO MOLAR FLOW [KMOL/H].	46
FIGURE 4.6 TEMPERATURE PROFILE AT CENTERLINE VS REACTOR LENGTH FOR STREAM 2E WITH $N_T = 708$. BLUE SOLID LINE: $T_{\text{in}} = T_{\text{cool}} = 508.35$ K, RED SOLID LINE: $T_{\text{in}} = T_{\text{cool}} = 508.55$ K, BLACK SOLID LINE: $T_{\text{in}} = T_{\text{cool}} = 508.15$ K.	49
FIGURE 4.7 SYNTHESIS LOOP WHEN A PURE H ₂ STREAM IS ADDED TO THE FRESH FEED MIXED WITH THE RECYCLE.	49
FIGURE 4.8 TEMPERATURE PROFILE FOR A REACTOR WITH AS FRESH FEED STREAM 2E AND THE ADDITION OF PURE H ₂ AFTER THE MIXING WITH THE RECYCLE.	51
FIGURE 4.9 LURGI CONFIGURATION ABOUT METHANOL SYNTHESIS [53].	52
FIGURE 4.10 LURGI METHANOL SYNTHESIS LOOP IN ASPEN HYSYS V 8.8.	54
FIGURE 4.11 TEMPERATURE PROFILE OF THE FIRST REACTOR FOR A LURGI CONFIGURATION WITH AS FRESH FEED STREAM 2E.	56
FIGURE 4.12 TEMPERATURE PROFILE OF THE SECOND REACTOR FOR A LURGI CONFIGURATION WITH AS FRESH FEED STREAM 2E.	56
FIGURE 4.13 TEMPERATURE AND PRESSURE PROFILE AT CENTERLINE VS REACTOR LENGTH FOR STREAM 2D WITH CONSTANT $R_i/N_T = 3.877$ KMOL/H PER EACH TUBE . BLUE SOLID LINE: TEMPERATURE, BLUE POINTED LINE: T _{COOL} , RED SOLID LINE: PRESSURE.	59
FIGURE 4.14 METHANOL AND CO MOLAR FLOW INSIDE THE REACTOR AT CENTERLINE, FOR THE STREAM 2D ADDING 1300 KMOL/H OF H ₂ .	61
FIGURE 4.15 TEMPERATURE PROFILE FOR A REACTOR WITH AS FRESH FEED STREAM 2D AND THE ADDITION OF PURE H ₂ AFTER THE MIXING WITH THE RECYCLE.	62

LIST OF FIGURES

List of Tables

TABLE 3.1 FRESH FEED AND REACTOR INLET COMPOSITION.	27
TABLE 3.2 REACTOR PARAMETERS	27
TABLE 3.3 RECYCLE PARAMETERS	31
TABLE 3.4 PB REACTOR MATERIAL BALANCE: CALCULATED VS MONTEBELLI ET AL. VALUES.	35
TABLE 3.5 PB REACTOR MATERIAL BALANCE: MONTEBELLI ET AL. [7] VS IMPROVED MODEL.	36
TABLE 4.1 PROPERTIES OF A STREAM COMING FROM THE REFORMING+ CO ₂ CAPTURE OF BIO-NG.	40
TABLE 4.2 PROPERTIES OF A STREAMING COMING FROM THE REFORMING OF BIO-NG.	40
TABLE 4.3 PERFORMANCES OF THE REACTOR WITH AS FRESH FEED STREAM 2E AND HIGHER FLOW RATIO IN THE SPLITTER.	43
TABLE 4.4 PERFORMANCES OF THE REACTOR WITH STREAM 2E AS FRESH FEED AND $RI/N_T = 3.877$ KMOL/H PER EACH TUBE.	44
TABLE 4.5 PERFORMANCES OF THE REACTOR WITH STREAM 2E AS FRESH FEED, $RI/N_T = 3.877$ KMOL/H PER EACH TUBE AND $T_{COOL} = 507.15$ K.	45
TABLE 4.6 PERFORMANCES FOR A REACTOR WITH STREAM 2E AS FRESH FEED AND $T_{IN} = T_{COOL} = 508.35$ K.	47
TABLE 4.7 PERFORMANCES FOR A REACTOR WITH STREAM 2E AS FRESH FEED AND 1) $T_{IN} = T_{COOL} = 508.15$ K; 2) $T_{IN} = T_{COOL} = 508.55$ K.	48
TABLE 4.8 PERFORMANCES FOR A REACTOR WITH AS FRESH FEED STREAM 2E WHEN DIFFERENT QUANTITIES OF PURE H ₂ ARE ADDED.	50
TABLE 4.9 PROCESS PERFORMANCES FOR THE LURGI CONFIGURATION WITH AS FRESH FEED STREAM 2E.	55
TABLE 4.10 PERFORMANCES FOR A REACTOR WITH STREAM 2D, WITH $RI/N_T = 3.877$ KMOL/H PER EACH TUBE.	60
TABLE 4.11 PERFORMANCES FOR A REACTOR WITH STREAM 2D WHEN DIFFERENT QUANTITIES OF PURE H ₂ ARE ADDED.	63

LIST OF TABLES

Nomenclature

\dot{q}	Heat flux [J/s]
$\Delta_R G^T$	Gibbs Free Energy of reaction at temperature T [J/mol]
$\Delta_R H^T$	Reaction Enthalpy at temperature T [J/mol]
A	Cross section area [m ²]
a_i	Activity of component i
B.C. _{RD}	Boundary conditions in radial direction [-]
B.C. _{RI}	Boundary conditions at reactor inlet [-]
$c_{p,g}$	Heat capacity at constant pressure for the gas phase [J/kg K]
D	Characteristic dimension [m]
d_P	Catalyst particle Diameter [m]
d_{PE}	Catalyst particle Diameter equivalent (as sphere) [m]
d_t	Tube diameter [m]
f	Fugacity [bar]
h_P	Catalyst particle height [m]
L_T	Tube length [m]
M_F	Fresh feed stoichiometric modulus [-]
M_I	Reactor inlet stoichiometric modulus [-]
Mw_i	Molecular weight of component I [kg/mol]
\dot{n}_i^{IN}	Molar Flow of component i at the reactor inlet [kmol/h]
\dot{n}_i^{OUT}	Molar Flow of component i at the reactor outlet [kmol/h]
N_T	Reactor Number of Tubes [-]
Nu	Nusselt' number [-]
P	Pressure [bar]
Pr	Prandtl number [-]
r	Tube radius [m]
$Re_{D_{pe}}$	Reynolds number referred to the equivalent diameter d_{PE} [-]
Re_p	Reynolds number for the particle [-]
R_{gas}	Universal constant of gas [J/mol K]
r_j	Rate of reaction for the reaction j [mol/kg _{CAT} s]
RR	Recycle Ratio [-]
T	Temperature [K]
T_{cool}	Reactor Temperature of the cooling medium [K]
$T_{HotSpot}$	Reactor Maximum Temperature [K]
T_{IN}	Reactor Temperature at the inlet section [K]
T_{React}	Reaction temperature [K]
U	Heat transfer coefficient [W/m ² K]
V_R	Reactor Volume [m ³]
v_s	Solid velocity [m/s]
y_{CO}	Carbon Oxide mole fraction [-]
y_{CO2}	Carbon Dioxide mole fraction [-]
y_{H2}	Hydrogen mole fraction [-]
y_{INERTS}	Mole fraction of inert compounds [-]
Z	Reactor axial dimension [m]

z°	Dimensionless Reactor Length [-]
η_j	Catalyst efficiency for the reaction j [-]
λ_{RAD}	Thermal Conductivity [W/m K]
μ	Dynamic viscosity [kg/m s]
ν_i	Stoichiometric coefficient of component i [-]
$\nu_{i,j}$	Stoichiometric coefficient of component i in reaction j [-]
ρ_{CAT}	Catalyst density [kg/m ³]
ρ_g	Gas density [kg/m ³]
φ	Void Fraction [-]
ϕ	Fugacity coefficient [-]
X	Conversion [-]
ω_i	Mass fraction of component i [kg/kg]

Glossary

Aspen HYSYS V8.8
Syngas
Bio_NG

Chemical Process Simulator by AspenTechnology
Fuel gas composed mainly of H₂,CO,CO₂
Fuel consisting of methane coming from renewable sources.

Tar
Char

Viscous liquid of hydrocarbons and free carbon.
Solid material that remains after the light gases and tar are remove from a carbonaceous material.

Estratto

Le fonti fossili sono state l'unica sorgente di energia per un lungo periodo. Il loro limite, che si contrappone all'elevata densità energetica, è la limitatezza: vi è una quantità finita disponibile che prima o poi si esaurirà. L'utilizzo delle fonti rinnovabili, in particolare le biomasse, per produrre energia è una delle nuove rotte su cui investire. La gasificazione delle biomasse a produrre Syngas e la successiva trasformazione dello stesso in metanolo, utile in svariati settori, potrebbe essere una risorsa importante nello scenario energetico presente e futuro.

L'obiettivo di questa tesi è fare una analisi delle performance di impianti "semplici" per la sintesi di metanolo, supponendo di alimentare ad essi syngas prodotto da biomasse attraverso differenti tecnologie. Per mezzo di simulazioni in Aspen HYSYS v8.8 si è cercato di ottimizzare le prestazioni dell'impianto su due particolari correnti (2E e 2D) con un coefficiente stechiometrico rispettivamente di 1.790 e 0.232. Senza tener conto dell'aspetto puramente economico le simulazioni riguardanti la corrente 2E hanno dato come risultato una produttività di metanolo di 262.50 kmol/h con una alimentazione di 828.6 kmol/h nella configurazione base, 277.20 kmol/h con la stessa precedente alimentazione a cui sono stati aggiunti (dopo il mix con il riciclo) 20 kmol/h di idrogeno puro e 266.10 kmol/h con la stessa alimentazione dei due casi sopracitati, ma utilizzando la configurazione Lurgi con due reattori in serie. Per quanto riguarda la corrente 2D, solo il caso in cui idrogeno puro viene aggiunto risulta in una accettabile produttività di metanolo. Quest'ultima è 607.56 kmol/h con una alimentazione di 1160 kmol/h ed una aggiunta di 1100 kmol/h di idrogeno. Lo scopo finale sarebbe applicare i risultati ottenuti in una valutazione economica dell'impianto e comprendere se è fattibile utilizzare questo procedimento per produrre metanolo.

Abstract

For a long time, non-renewable energy sources were the only way to produce energy. Their limit, which contrast with their high energy density, is the finiteness: they will dwindle until eventually disappear. The interest to invest in renewable sources, such as biomasses, is increasing over the years. The gasification of biomasses producing syngas and its transformation into methanol, a very versatile molecule, can be an interesting route in the present and future energy scenario.

The aim of this thesis is to analyse the performance of “simple” plants for the production of methanol, supposing to feed them with syngas produced from biomasses through different technologies. By means of simulations in Aspen HYSYS v8.8, the performances of the process loop with as fresh feed two different flows (2E and 2D) with the stoichiometric coefficient respectively 1.790 and 0.232 have been optimized. Without considering the economical aspect, the simulation performed on the stream 2E brought as result of the methanol productivity 262.50 kmol/h with 828.6 kmol/h as fresh feed, 277.20 kmol/h for a fresh feed equal to the previous one where 20kmol/h of pure hydrogen have been added (after the mixing with the recycle) and 266.10 for the same fresh feed as in the first case but with two reactors in series (Lurgi configuration). Regarding the stream 2D, just the simulation that involved an addition of pure hydrogen can be considered acceptable. With a fresh feed of 1160 kmol/h and 1100 kmol/h of hydrogen added, the methanol productivity results 607.56 kmol/h. Purpose of this work is to give the base for a profitability assessment in order to understand whether or not methanol can be produced with this method.

Preface

Methanol is an important compound used in many different ways. Its production starting from renewable sources could be a new route in order to erase the world dependence from fossil fuels.

In this work we adapt the design of a multitubular reactor with heat exchange, based on the one modelled by [7], to several fresh feed compositions that are the results of the biomasses gasification.

Trough simulations, this work optimizes the methanol yield varying design parameter (such as number of tubes, inlet temperature of the reactor, coolant temperature in the reactor, purge extent) and observing the behaviour of hotspot temperature, inerts content in the reactor inlet, recycle ration and stoichiometric coefficient at the reactor inlet.

The remainder of this paper is organized as follows: chapter 1 provides a theoretical background and a research literature on biomass gasification. Chapter 2 explains the basic principles of the process simulator used in this work, Aspen HYSYS V8.8 [8,9]. Chapter 3 describe in detail the simulation model of the process under investigation and the validation process we performed. Chapter 4 discusses the behaviour of the plant obtained from the numerical simulations with different operating conditions. Multiple cases with different fresh feed compositions have been evaluated to understand whether it is possible to create methanol in a reasonably quantity starting from an inlet stream with properties not close to the designed ones (e.g. a stream with a stoichiometric coefficient at the reactor inlet not in the range of the optimal one). Furthermore, in this chapter we study a new configuration involving two multi-tubular reactors in series to achieve the optimal temperature profile. We draw some conclusions and think about possible future works in Chapter 5

1

Introduction

The world total energy demand is about 400 quadrillion British Thermal Units — or BTUs — each year (Source: US Department of Energy). Fossil fuels, e.g. oil, coal and natural gas, supply nearly 88 percent of the world’s energy needs. However fossil fuels are non-renewable, that is, they draw on finite resources that will eventually dwindle, becoming too expensive or too environmentally damaging to retrieve. Furthermore, fossil fuels are considered to be the largest contributing factors of global warming and environmental pollution due to the greenhouse gas emissions. On the other hand, renewable energies, e.g. wind and solar energies, are constantly replenished and will never run out [1] and can play an important role in the improvement of the atmospheric health. As shown in Figure 1.1 there are different types of renewable energies according to the energy source:

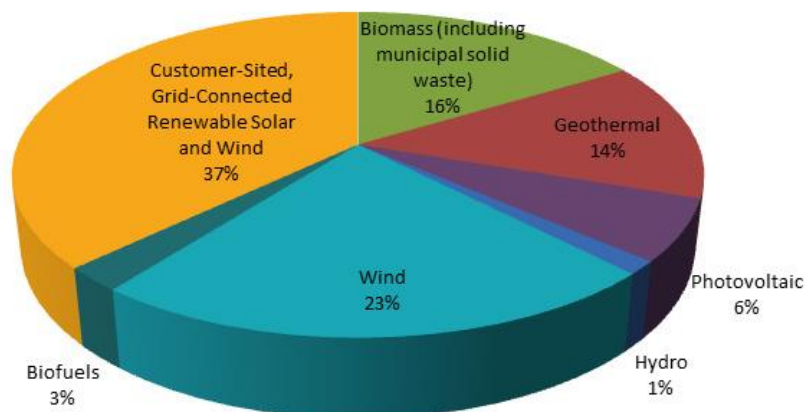


Figure 1.1 Types of Renewable Energy [2].

INTRODUCTION

- Solar energy can be used for heating purposes in both residential and industrial services;
- Wind energy, captured with wind turbines, coupled with the sun's heat, evaporates water. The latter then falls as rain or snow into rivers or streams, capturing energy as hydroelectric power;
- Hydrogen can be found on organic compounds and it is the most abundant element on the earth. This element can be burnt as fuel or converted into electricity;
- Geothermal energy taps the Earth's internal heat for a lot of uses as heating power, electric power and cooling power;
- Ocean energy, such as waves energy, tidal energy etc;
- Biomass, that is the organic matter that makes up plants. Biomass energy can be used for various scope becoming then bioenergy.

Solar and Wind power are in principle able to satisfy the overall world energy demand [2]. The difficulties of relying on these renewable energies are related to the volatile power feed due to the nature of the sources that are not linked to the power needs. It is not possible to completely rely on them. Their variance, though, can be smoothed by using other energy sources e.g. Biomasses energy. Biomasses are largely available and can be stored. On the other hand, the main problem is that biomasses have a very low energy density, yielding to a necessary transformation into something more applicable.

INTRODUCTION

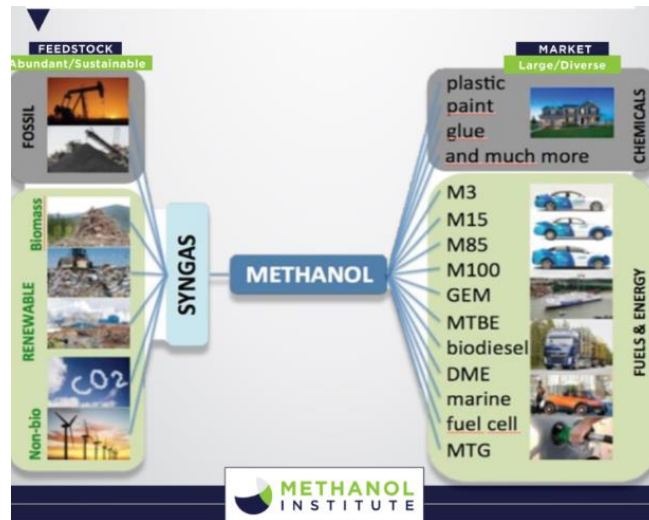


Figure 1.2 Methanol provenience and usage [3].

This something can be a liquid fuel, like methanol, that is one of the most versatile molecule. Figure 1.2 shows that methanol is used to produce other chemical derivatives, which in turn are used to produce thousands of products that touch our daily lives, such as building materials, foams, resins, plastics, paints, polyester and a variety of health and pharmaceutical products. Methanol also is a clean-burning, biodegradable fuel [4].

Moreover, due environmental and economic advantages, methanol is becoming an attractive alternative fuel for powering vehicles and ships, cooking food and heating homes. Figure 1.3 shows that methanol demand hence methanol production is increasing over the years.

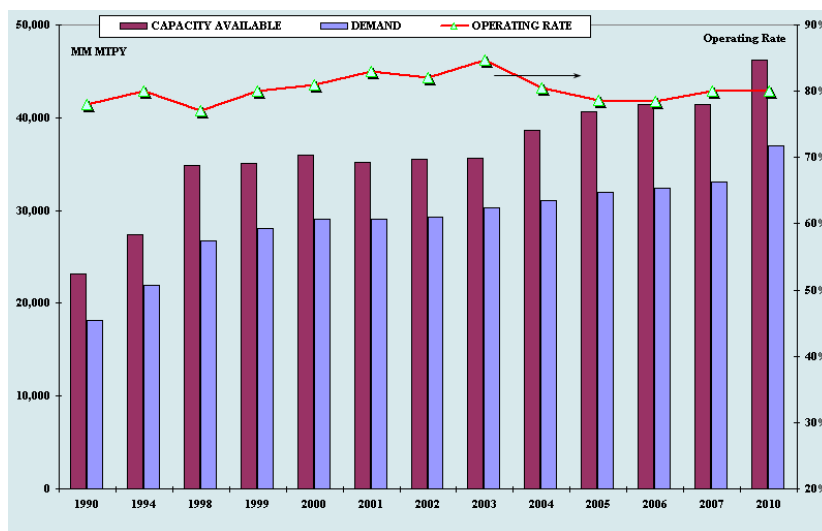


Figure 1.3 Methanol Demand and Production [5].

INTRODUCTION

As introduced before, to really exploit the energy potential of biomasses, their transformation into methanol is needed. Once they are gasified to obtain syngas, the latter will be used to synthesized the final product.

Figure 1.4 shows the plant scheme to convert a stream rich of CO, CO₂ and H₂ to CH₃OH.

The fresh feed (stream 1) has to be compressed. Starting from ambient pressure, the goal one will be at least 60 bar (stream 2). Hence, more than one unit operation, coupled with intercooler (to avoid excessive increase of temperature) is needed. Subsequently, the pre-heater, used to bring the reactants to the desired inlet temperature (stream 4), and the reactor, main unit operation in which the conversion from CO_x to methanol is performed, are implemented. The stream coming out from the reactor (stream 5) pass through a cooler that will decrease the temperature helping in a more efficient separation performed in the flash (stream 6). At the very end, the vapor stream coming out from the separation section (stream 8), after a small purge (stream 9), will be recompressed (stream 11), recycled back and mixed with the fresh feed in order to increase the overall methanol yield (stream 3). The liquid coming out from the flash (stream 7) will be a mix of mainly methanol and water.

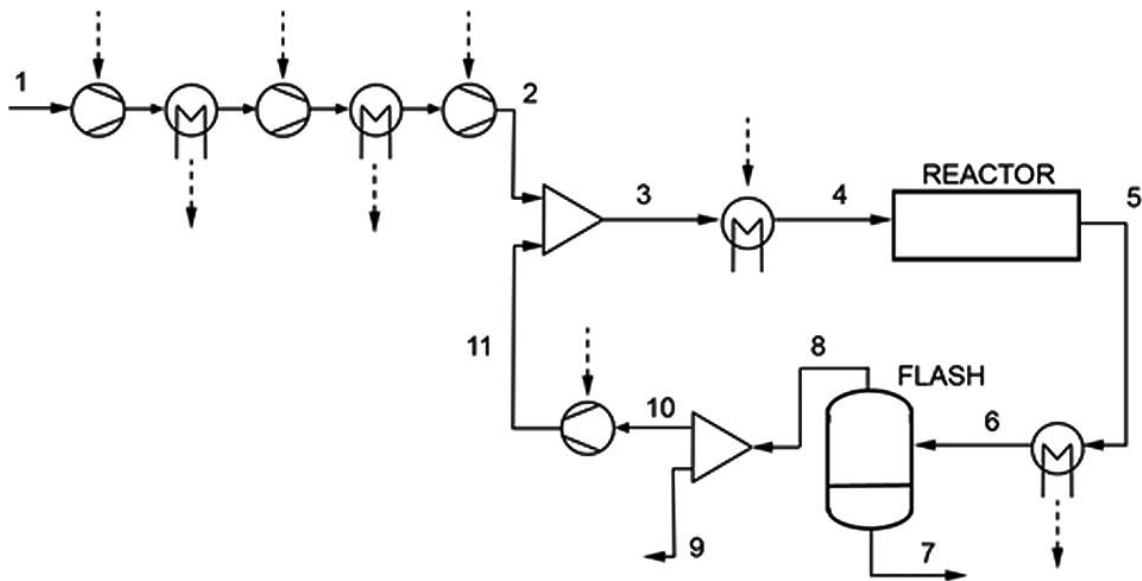


Figure 1.4 Methanol Synthesis Loop [6].

INTRODUCTION

1.1 Theoretical Background

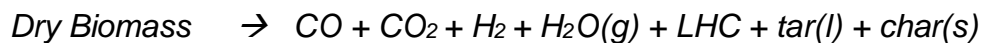
This chapter explains all the necessary theoretical aspect behind the whole process to transform biomass to methanol. The first step is the gasification of biomass to syngas that will be followed by the methanol synthesis.

1.1.1 Biomass gasification

Biomass is usually a dry solid and can be both gasified or burnt. In 2015 almost 82% of the total biomass content was used in the energy sector for transportation, house services and industries [10,11]. The gasification process transforms into gaseous phase liquid or solid feed-stream. A quick overview of the process is here described:

Drying Endothermic process that involve an evaporator to eliminate the water percentage in the biomass. The higher is the humidity, the higher will be the heat needed.

Pyrolysis Thermal decomposition of the completely dry biomass in a range of temperature going from 270°C to 700°C. This is a chemical endothermic reaction that follows the scheme:

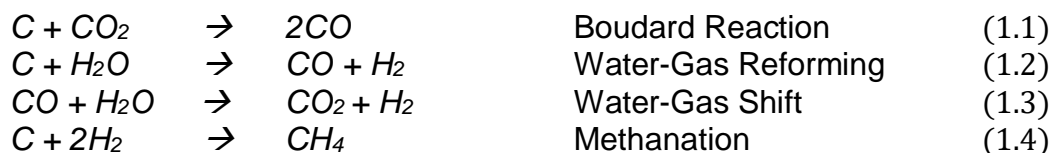


Oxidation Chemical step that is mainly used to produce the heat of reaction that has to be supplied for the other steps. It follows the scheme:



INTRODUCTION

Reduction The chemical compounds created during the previous phase are mixed and react together forming other products. The main reactions, overall endothermic, are [12,13]:



A variety of compounds can be produced from these reactions. Changing the temperature range will change the selectivity toward one or more components. 800°C-1100°C (500°C-1600°C) are the temperatures used in biomass gasification in air (O₂) in order to achieve the syngas production [14].

To better understand the procedure, including operations involved to clean the gas produced and all the facets of the four steps it is suggested the reading of [15].

1.1.2 Methanol Synthesis

The first methanol molecule was produced in 1661 by Robert Boyle via rectification of crude wood vinegar over milk of lime. Then only in 1913 the first commercial methanol synthesis process was patented by Alwin Mittasch at BASF starting from CO and H₂ in the presence of Iron as catalysts. Problems of this configuration were contamination by Fe, Ni, S, catalyst active only at very high T (thus very high P) and methanation as side reaction. Continuing on the timeline, changes of catalyst and operating conditions were applied improving performances (ICI Process 1966-1972 with Cu/ZnO/Al₂O₃ or Cu/ZnO/Cr₂O₃ as catalyst active at T = 200 - 250°C and P= 150-200 atm) [16].

Methanol (CH₃OH) is a compound soluble in water, alcohols and organic compounds with a boiling temperature of 64.6 °C and a melting temperature of -98 °C. The most important properties that has to be kept in mind during its synthesis are the flammability limits in air (6.7 – 36.5 % v/v) and its toxicity [16].

INTRODUCTION

Reaction scheme:



Thermodynamic effect

The overall reaction is exothermic and with a decreasing number of moles. Decreasing the temperature, the Keq increases, decreasing the pressure, the equilibrium conversion decreases.

T, °C	Keq
260	1.5×10^{-3}
300	3.1×10^{-4}
340	8.7×10^{-5}
80	2.7×10^{-5}

P [bar]	Eq. χ
250	60 % ca.
10	2 % ca.

Where χ and Keq can be calculated with:

$$\chi = \frac{\dot{n}_i^{IN} - \dot{n}_i^{OUT}}{\dot{n}_i^{IN}} \quad (1.8)$$

$$Keq = e^{-\frac{\Delta_r G^T}{RT}} = \prod a_i^{v_i} \quad (1.9)$$

Stoichiometric Effect

As Figure 1.5 display, changing the composition of the feed of a methanol synthesis reactor will bring changes in the product composition, hence in the methanol productivity. The parameter used in order to establish the quality of the inlet stream is:

$$M_i = \frac{y_{\text{H}_2} - y_{\text{CO}_2}}{y_{\text{CO}} + y_{\text{CO}_2}}$$

A suitable value for M_i is in the range of 2.0 - 2.2, indicating an excess of hydrogen that will be recycled back.

INTRODUCTION

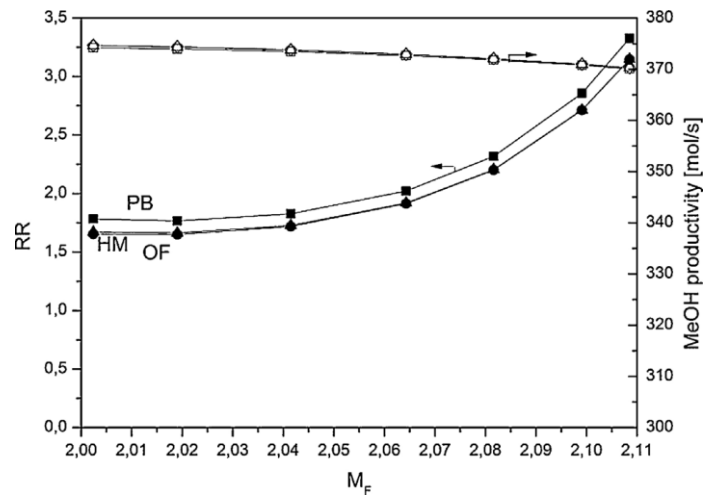


Figure 1.5 Methanol productivity and Recycle Ratio vs M_F [7].

Kinetic Effect

Looking at Figure 1.6 it can be seen that the reaction rate increases with the temperature due to the Arrhenius effect, when no methanol is present in the mixture. As soon as some products are present, the reverse reaction starts. The latter is an overall endothermic step that is favoured at higher temperatures and that lead to a decrease in the methanol concentration. All the methanol synthesis reactor works with a temperature profile that is decreasing with its length. When $z = 0$, no methanol is present and it is possible to work with the maximum allowable temperature that corresponds to the maximum allowable reaction rate. Increasing z , methanol concentration increases, leading to an activation of the aforementioned reverse reactions. At this point, the maximum allowable reaction rate will be encountered at different decreasing temperatures.

INTRODUCTION

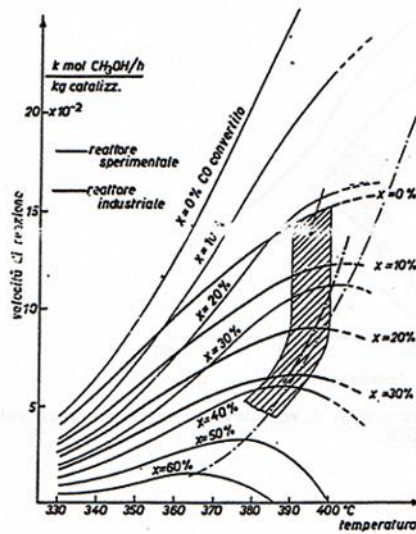


Figure 1.6 Methanol reaction rate vs Temperature [17].

Catalysis effect

What is important to achieve during methanol synthesis is a good value of selectivity toward methanol. To accomplish this task, a catalyst is needed, in order to speed up the main reactions and avoid the production of by-products. Some of the side reactions that have to be controlled are:

Methanation



Dehydration



Higher Alcohols



Oxygenates



The most dangerous one is the methanation reaction, not only because from methanol we go back to syngas (the starting reactants) but also because of its

INTRODUCTION

exothermicity that makes the system really unstable with the possibility of thermal runaway. To block (1.8) it is necessary to keep the temperature below 270°C [17].

1.2 State of the art

The aim of this chapter is to report all the different technology to produce syngas, and successively methanol, starting from renewable sources. Methanol is one of the most important intermediates in the chemical industry. It can be used as substituent/supplement in the traditional fuels for internal combustion engine or to produce oxygenates and hydrocarbons [18,19].

1.2.1 Bio-Syngas Production

The gasification of biomass to produce syngas will be a key technology for the production of biofuels [20, 21]. In particular the technology that employ entrained flow gasification of biomass allows the manufacturing of high quality syngas that can lead to different types of biofuels [22]. The main disadvantage of this methodology is the elevated temperature, in the range of 1200-1300°C, needed to achieve high carbon conversions with short residence time, that leads to soot formation [23, 24]. Moreover, the high yield to ashes can cause accumulation in the reactor unit and plugging of its outlet flows [25, 26, 27]. To make this process competitive, some study about the impregnation of biomass with alkali metals were pursued [28, 29] and they led also to reduced tar formation [29]. The other advantage brought from the alkali impregnation is the decreasing of the temperature and the use of the alkali as flux agent increasing the ability to flow of the total mixture [25, 26, 27, 30]. Of course, adding alkali metals has a cost that

INTRODUCTION

has to be considered in the profitability assessment of this investment. When gasification is adopted, there are two main purposes: to convert all the possible raw material into gas and to maintain stable its properties [31]. The gas is formed mainly by H_2 and CO with a percentage of CO_2 depending on the different technology used before and after the gasification [32]. Of course, the gasification extent depends on a lot of parameters. [33] asserted that biomass composition can depend on the age of the plant, growth processes, if fertilizer and pesticide were used and in what quantity, harvesting time, pollution, moisture percentage and type. Precisely there are three types of moisture that can be present in a biomass: Surface moisture, chemical moisture, moisture on air/steam. Moisture content in a biomass can range from 30% to 90% [34]. As [35] write, anaerobic digestion can be applied in order to stabilize toxic and dangerous waste. Even though the biogas produced from this mechanism is mainly methane, it also contains the right compounds for the methanol synthesis [36].

1.2.2 Methanol Synthesis

Methanol synthesis is a well-studied process. Normally it is carried out on a catalyst of $CuO/ZnO/Al_2O_3$ at a temperature around 250-300 °C realising 50 KJ/molMeOH [7]. The selectivity of these processes can reach value of 99.9 % [37] but yield (thus Conversion) is limited by thermodynamic equilibrium. Conversion for a once-through configuration is in the range of 20% while considering the recycle of the reactor effluents (after a small purge) allows to reach value of conversion next to 80% [38, 39]. Disparate reactor design can be applied to this configuration (fixed bed reactor, bubble reactor, fluidized bed reactor) but the best ones are the fixed bed reactors with quench (Figure 1.8) or multitubular reactor with an external cooling [40].

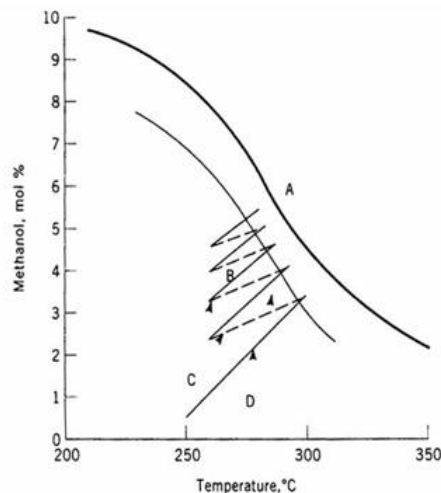


Figure 1.7 Profile of Methanol conversion vs Temperature for a Quench reactor [17].

INTRODUCTION

The former design configuration is performed as a series of fixed adiabatic bed reactor where at the inlet of each stage fresh syngas is injected to cool down the stream, allowing to better follow the optimal temperature profile maximizing the reaction rates (Figure 1.7).

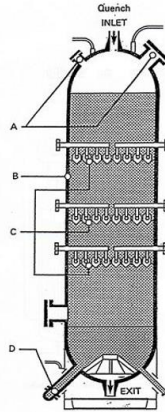


Figure 1.8 Design of a Quench reactor [15].

In Figure 1.9 is shown a multitubular reactor. This is a quasi-isothermal reactor with a tubular bundle and a shell. In one of two parts circulate the process flow (usually inside the tubes) and in the other the cooling medium (usually in the shell) that for these temperatures can be assumed as water. This will be the technology simulated in our work, its methanol concentration and temperature profile will be displayed in the following chapters. Main advantages of this technology compared to the previous one is that the recovery of the heat realised from the reaction is possible, higher yield and higher lifetime for the catalyst adopted are reachable but, on the other side, its operating and capital costs are higher [16]. Lurgi, Johnson Matthew/Davy and Haldor Topsøe are the market drivers [41].

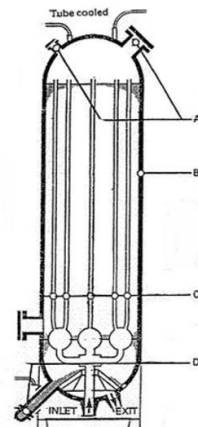


Figure 1.9 Design of a Multitubular reactor [17].

INTRODUCTION

2

Materials and Methods

As previously mentioned, all the simulations were carried out within the process simulator Aspen HYSYS V8.8. The aim of this chapter is to describe the basic principles of Aspen HYSYS.

Figure 2.1 shows an example of simulation model of the methanol synthesis process in Aspen HYSYS. Following the unit operations will be explained.

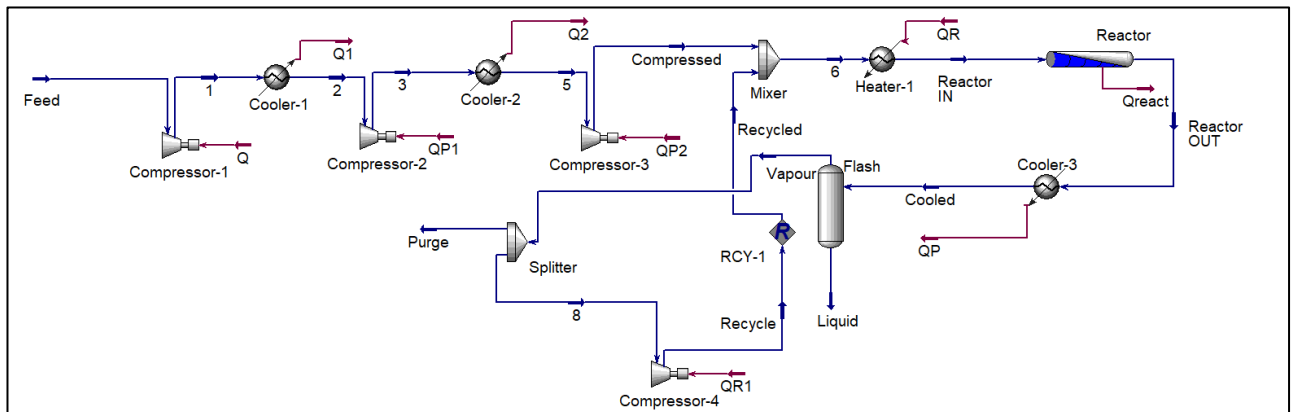


Figure 2.1 Methanol Synthesis loop in Aspen HYSYS V8.8.

MATERIAL AND METHODS

2.1 Setting the environment

The first thing to start a simulation in Aspen HYSYS V8.8 is to set the properties environment as in Figure 2.2. This means that all the component involved in the model have to be declared and specified.

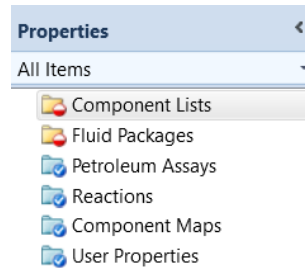


Figure 2. 2 Set of the environment in Aspen HYSYS.

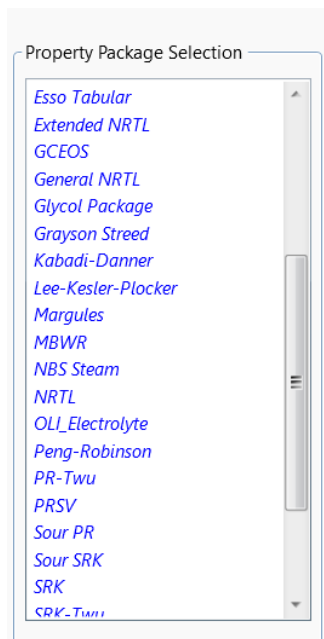


Figure 2.3 List of Fluid Packages.

Aspen HYSYS has a library incorporated in which a number of elements and compounds with their properties are already specified and this allows avoiding the tedious work of searching them in literature. If one or more components are not present in the library, a tool to specify the name and some of its properties is present. Once all the component will be specified the fluid package has to be added. A variety of them are already present in Aspen HYSYS library (Figure 2.3) but, as before mentioned, also in this case it is possible to a customized package. The method assistant tool will help in the decision of the fluid package to attach.

In our work, the fluid package to attach will be the RKS. Looking at [15,16], this fluid package is the most accurate if used in simulation regarding Oil&Gas and derivatives industries.

MATERIAL AND METHODS

2.2 Process streams

Once the properties environment is fixed (one can always add something forgotten during the next steps), the simulation environment can be open and the real design phase starts. Figure 2. 4 shows three types of arrows, respectively the light blue one (prephase of the dark blue) is used to indicates process streams while the purple one indicates energy streams.

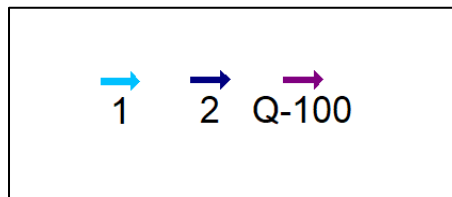


Figure 2.4 Process and Energy streams.

Double click on them and a window appears in which properties can be specified. For the process stream at least 3 independent properties and the composition have to be declared to completely define the stream (Figure 2.5) and change its colour to blue.

Worksheet	Attachments	Dynamics
Worksheet	Stream Name	1
Conditions	Vapour / Phase Fraction	1.0000
Properties	Temperature [C]	22.00
Composition	Pressure [kPa]	3.000
Oil & Gas Feed	Molar Flow [kgmole/h]	<empty>
Petroleum Assay	Mass Flow [kg/h]	4.000
K Value	Std Ideal Liq Vol Flow [m3/h]	<empty>
User Variables	Molar Enthalpy	<empty>
Notes	Molar Entropy [kJ/kgmole-C]	<empty>
Cost Parameters	Heat Flow [kJ/h]	<empty>
Normalized Yields	Liq Vol Flow @Std Cond [m3/h]	<empty>
	Fluid Package	Basis-1
	Utility Type	

Figure 2.5 Process stream worksheet.

The energy stream is usually coupled with a unit operation that requires or produces energy while running. The direct value for the energy per hour

MATERIAL AND METHODS

transferred or a formula involving correlation between variables are present. Energy can be transferred via direct power or with medium called utility fluid.

2.3 Compressors

Compressors are used to increase the pressure of a process streams. As it can be seen from Figure 2.6 compressors have three phases:

1. The red one in which no streams are attached and no operation can be done.
2. The grey with yellow contour in which all the process and energy streams are attached but no clue about how much we have to increase the pressure has been declared.
3. The grey with the blue contour is when all the necessary data are given and the compressor simulation is completed.

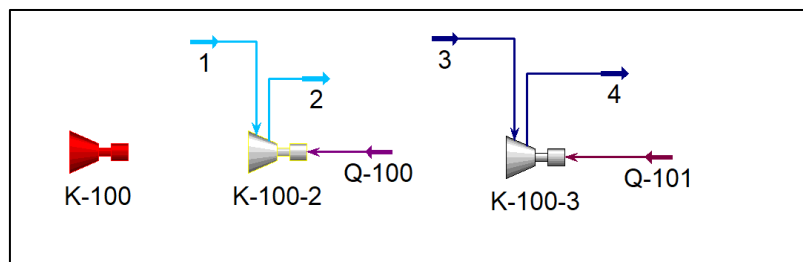


Figure 2.6 Three phases of a compressor.

Actually, these three phases can be seen in all the unit operation (relating them to the variable they need) involved in a process loop.

Once all the inlet process streams are defined, there are two different ways of completing the simulation of a compressor:

- Providing the Duty that the compressor has to use in order to accomplish its job;
- Providing the Pressure of the outlet stream.

As Figure 2.7 displays, there are a number of variables already fixed automatically from the simulator but they can be changed if necessary.

MATERIAL AND METHODS

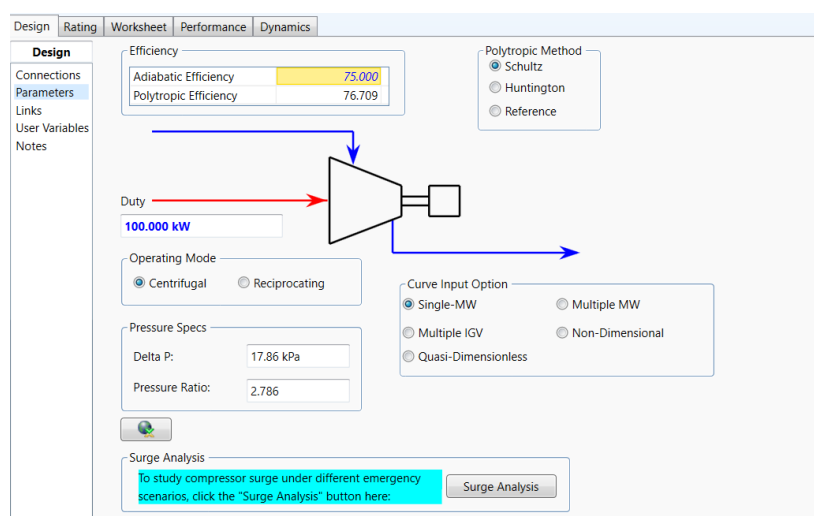


Figure 2.7 Compressor parameters.

In our work it has been used a polytropic efficiency equal to 0.98. Considering the viscosity of the fluids passing through the compressors, 0.98 is a well assumed value that indicate a small loss in terms of “work” that identify a small additional heating.

2.4 Coolers and Heaters

Coolers/Heaters (Figure 2.8) are used to decrease/increase the temperature of a process streams. In aspen HYSYS their icons are very similar, but they can be recognised from the direction of the energy stream: for a cooler the energy stream is going away and the opposite for a heater. What it has to be done to complete the simulation of these two unit operation, once the inlet process stream is defined, is to fix at least two parameters choosing between:

- Duty exchanged
- Pressure Drop → Always assumed 0 to avoid any additional loss of pressure
- Outlet temperature
- Outlet pressure.
- ΔT between inlet and outlet temperature of the process stream

MATERIAL AND METHODS

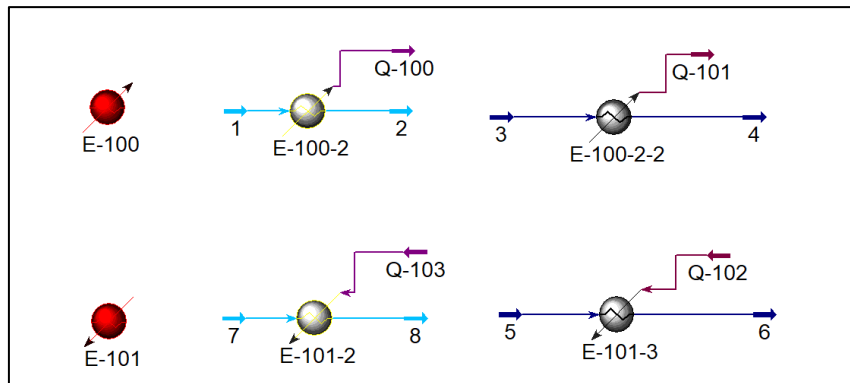


Figure 2.8 Coolers and Heaters.

2.5 Mixer and splitter

Mixer/splitter is a unit operation used to mix/separate two or more process streams, without influencing their composition. The former needs, besides the definition of the inlet streams, just its rating (diameter and elevation from the ground), while the latter needs also the ratio with which the streams are separated. Other specification can be added to both of them in case of an economic assessment or an energy optimization. Figure 2.9 shows the Aspen HYSYS icons relative to these unit operation.

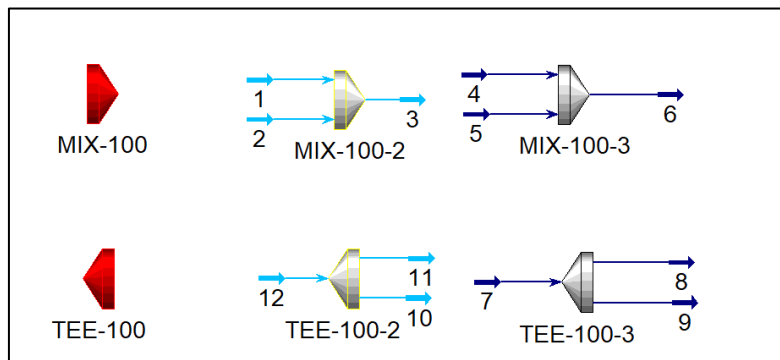


Figure 2.9 Mixer and Splitter.

MATERIAL AND METHODS

2.6 Reactor

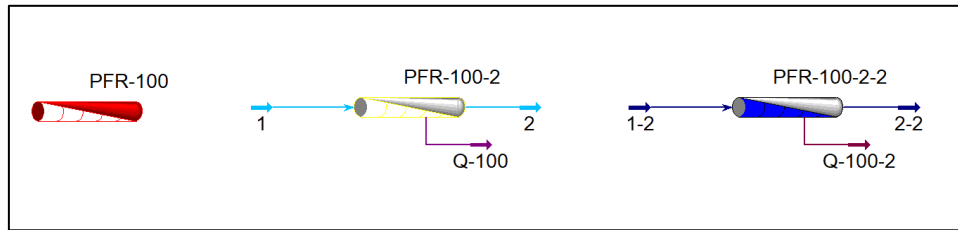


Figure 2.10 Reactor.

Figure 2.10 exhibit a PFR reactor with tubes inside. The process stream flows in the tubes, instead the cooling water is in the shell. First thing to do is to add a reaction to the reactor. Typing back on the property environment it is possible to decide what type of reaction to use. In this case a heterogeneous catalytic reaction set is added as in Figure 2.11. This set require all the kinetic data that will be described in the next chapter. Once a reaction set is attached to the fluid package it is possible to continue with the simulation of the reactor.

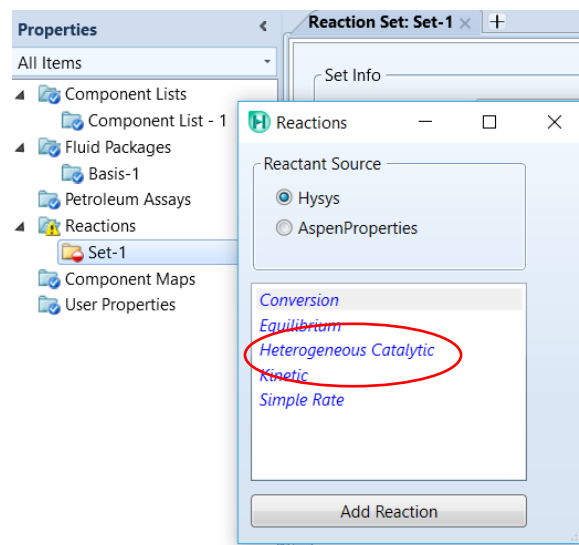


Figure 2.11 Reaction set attachment.

Next step will be the dimensions of the reactor. This include its length and diameter in order to find the volume, N_T , tube diameter, wall thickness and void fraction regarding the tube packing. Catalyst particle properties have to be known as well, because sphericity, density and d_p are parameters involved in the

MATERIAL AND METHODS

reaction rate calculation. In the end, duty information (direct Q value or correlations about it) and pressure drop information (in which not only a number can be included but also the Ergun equation can be used) will allow the complete simulation of the reactor. In this unit operation a lot of variables are fixed by Aspen HYSYS, it is suggested to go through all the windows available because some other important parameters, such as T_{cool} or iteration points, could be different from what it is needed.

2.7 Flash

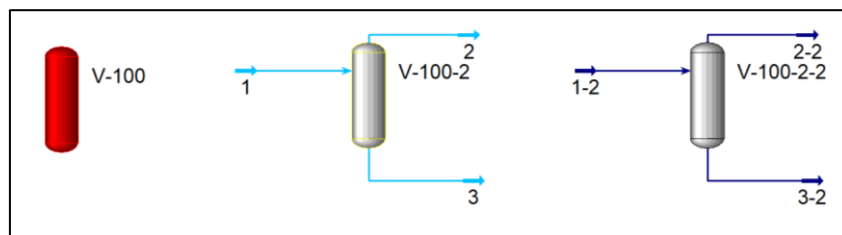


Figure 2.12 Flash.

The flash (Figure 2.12) is a unit operation that performs a separation in two different phases (liquid and vapor) between compounds in the same process stream. It can involve a reaction or not, it can be subject to pressure drop or not, it can be isothermal or with changing temperature (in this case an energy stream is required). To completely define a flash, its inlet flow has to be defined as well. As in the other unit operation whose performances do not depend on the size, Aspen HYSYS will automatically fill rating properties that can then be changed if necessary.

In our work, the temperature of all the three streams (one entering and two exiting) the flash are at the same temperature. No pressure drop is considered in the simulation and the liquid percent inside the flash is never higher than 50%. With these assumptions, that allows us to simplify the problem, the flash simulation is a mere separation that follows the affinity of the components to either vapor or liquid phase.

2.8 Recycle Operator

The operator shown in Figure 2.13 is something you need when a recycle is inserted in the loop in order to reach convergence. Sensitivity, tolerances, number of steps, maximum number of iterations and numerical method are just some of the specifications that Aspen HYSYS fixes instantaneously but that can be changed to adapt them to the problem.

MATERIAL AND METHODS

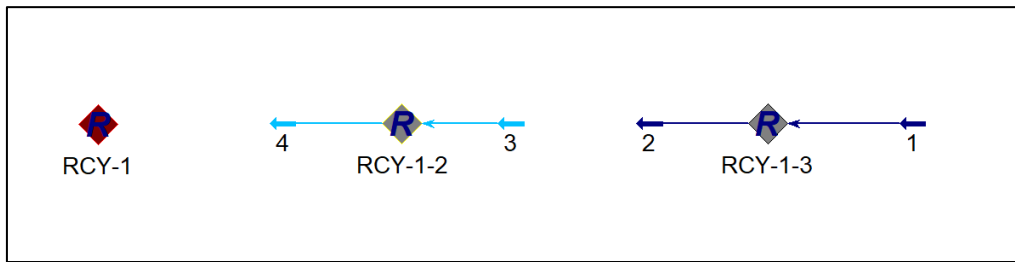


Figure 2.13 Recycle Operator.

This is the most important unit operation in the Aspen HYSYS simulation. When a recycle is inserted in a loop, convergence problem usually appears. By means of adjust operators (tool that help you reach a fixed value for a variable, changing the value of another one) and of spreadsheets (tool that allows to fix a formula or a relationship between variables and configure your simulation on these relationships), the recycle can be handled in a simpler way and kept under control.

2.9 Component Splitter

The unit operation in Figure 2.14 is not visible in the loop presented by Figure 2.1 at the initial paragraph of this chapter but it will be useful in the validation of the initial model. The purpose is to split components of one process stream, between two phases (liquid and vapor) not considering their affinity to one of the two phases but forcing them into the one you are interested in. This unit will be useful to represent an ideal flash in which the outlet stream of the methanol reactor will enter. The liquid product will be composed of only methanol and water, while the vapor one will contain all the other compounds.

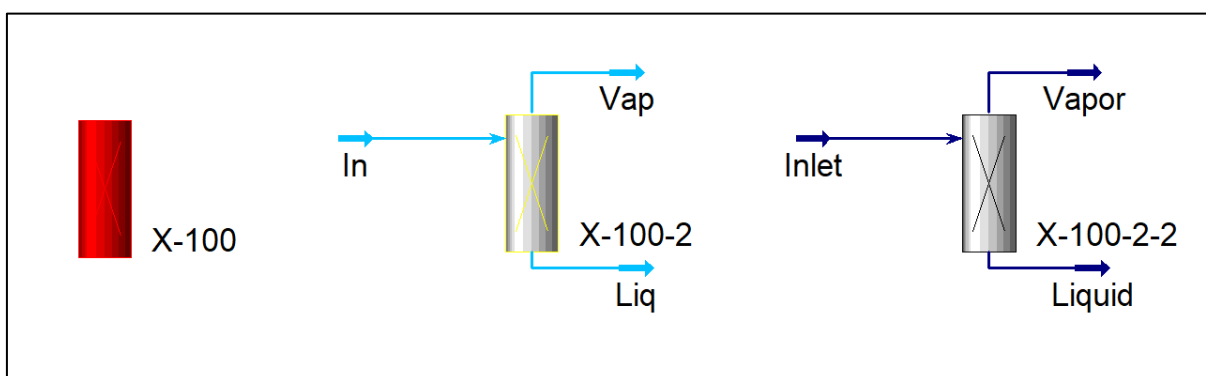


Figure 2.14 Component Splitter.

To simulate this unit operation first of all splits ratios have to be defined. This is the core information, because all it is needed is to tell where one component will go. Also, an energy stream can be added in case of non-isothermal separations.

MATERIAL AND METHODS

If this detail is not known, temperature, vapor fraction, pressure and enthalpy of the outlet streams can be specified to fill the last degree of freedom.

In our work the pressure of all the streams involved in this unit is equal, as well as their temperature. In this way, the state equation of enthalpy and entropy are easily calculated and the separation between compounds quickly performed.

MATERIAL AND METHODS

3

Model Building and Validation

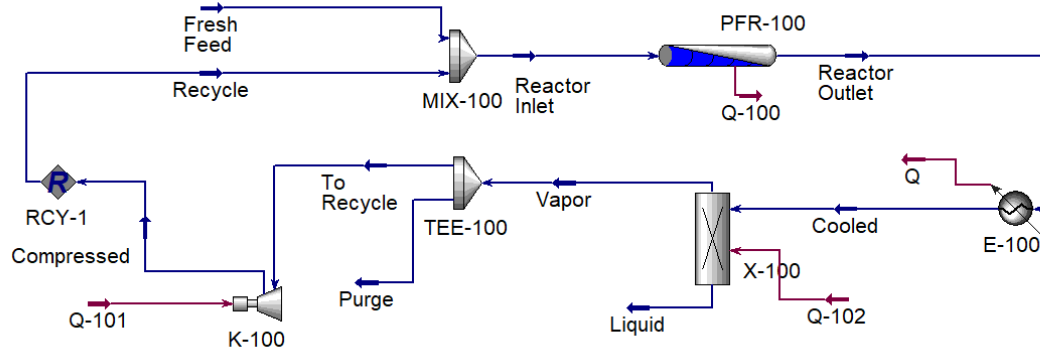


Figure 3.1 Methanol synthesis loop [7].

Figure 3.1 shows the synthesis loop used by [7] in their work. To validate the model a simulation based on their data was performed. In this Chapter equation used and all the necessary information about the model will be displayed. A comparison between the model developed and the one proposed by [7] will be displayed and highlighting our improvements to better follow real case process data.

3.1 Assumption

- Axial and radial dispersion in the mass balance are neglected.
- In this work, the reactor is a 2-D steady-state heterogeneous pseudo-continuous reactor. Only the gas phase was modelled, neglecting the modelling of the solid phase. This is a huge hypothesis to do, but it is not possible to include the modelling of the solid phase in Aspen HYSYS.
- Due to the impossibility to include the formula regarding the catalyst efficiency, an average value has been used in the reaction kinetics based on the work of [42] and on the operating conditions applied to this loop. This simulation was also compared to the one with a unitary catalyst efficiency and the result are comparable.
- There is no possibility to fix the inerts content in the reactor inlet as [7] did, what it can be done is to fix the purge ratio in a way that the numbers correspond. To do so all the types of inerts are collected as Methane, neglecting the presence of Argon and Nitrogen. Even though their heat capacities are different, the results are not affected by this assumption.
- The Temperature of the cooling medium is constant, it does not change between inlet and outlet. To simulate this, the flow rate of the cooling medium has been set at a very high value.
- The radial resistance to the heat exchange carried out by the wall is neglected.

MODEL BUILDING AND VALIDATION

3.2 General Data

The general operating conditions for the process loop are displayed in Table 3.1. Composition of the fresh feed and inerts content at the reactor inlet are already known, as well as temperature and pressure of both fresh feed and reactor inlet. The molar flow rate of the reactor inlet is fixed while the fresh feed flow rate is inferred.

	FF	RI
y_{H_2}	0.6864	Unknown
y_{CO}	0.2732	Unknown
y_{CO_2}	0.0355	Unknown
y_{CH_4}	0.0049	0.0082
y_{CH_3OH}	0.0	Unknown
y_{H_2O}	0.0	Unknown
\dot{n}_{TOT} [Kmol/h]	4360	18030
T [K]	323	323
P [bar]	69.20	69.20

Table 3.1 Fresh Feed and Reactor Inlet Composition.

3.3 Reactor section

	Input value
N_T	4650
φ	0.387
d_{PE} [mm]	4.85
ρ_{CAT} [Kg/m ³]	1714
T_{cool} [K]	511
d_t [m]	4.2×10^{-2}
d_P [m]	6.0×10^{-3}
h_P [m]	3.5×10^{-3}
L_T [m]	8.0
V_R [m ³]	51.54

Table 3.2 Reactor parameters

MODEL BUILDING AND VALIDATION

Table 3.2 shows all the necessary data to simulate the reactor. The latter is a Multitubular reactor that uses as cooling medium water at a constant temperature. Inside the tubes, the process stream flows through the catalyst pellets. Their shape is cylindrical but an equivalent spherical diameter to consider them as sphere and allow a simpler simulation has been used.

The balance equation for the reactor are:

$$\frac{\dot{n}_{TOT}}{A} \cdot \frac{d\omega_i}{dz} = Mw_i \cdot (1 - \phi) \cdot \rho_{cat} \cdot \sum_j v_{i,j} \cdot \eta_j \cdot r_j \quad (3.1) \quad \text{Mass Balance}$$

$$\omega_i(z = 0, r) = \omega_i^{IN} \quad (3.2) \quad \text{B.C.}_{RI}$$

$$c_{p,g} \cdot \frac{\dot{n}_{TOT}}{A} \frac{dT}{dz} = \lambda_{RAD} \cdot \left(\frac{d^2T}{dr^2} + \frac{1}{r} \frac{dT}{dr} \right) + (1 - \phi) \cdot \rho_{cat} \cdot \sum_j (-\Delta_R H_j) \cdot \eta_j \cdot r_j \quad (3.3) \quad \text{Enthalpy Balance}$$

$$T(z = 0, r) = T^{IN} \quad (3.4) \quad \text{B.C.}_{RI}$$

$$\frac{dT(z, r = 0)}{dz} = 0 \quad (3.5) \quad \text{B.C.}_{RD}$$

$$\dot{q} = \lambda_{RAD} \cdot \frac{dT(z, r = r_0)}{dr} = U_{TOT} \cdot (T_{cool} - T(z, r = r_0)) \quad (3.6) \quad \text{B.C.}_{RD}$$

$$\frac{dP}{dz} = - \left(1.75 + 150 \cdot \frac{1 - \phi}{Re_p} \right) \cdot \frac{1 - \phi}{\phi^3} \cdot \frac{\rho_g \cdot v_s^2}{d_p} \quad (3.7) \quad \text{Ergun Equation}$$

$$Re_p = \frac{\rho_g \cdot v_s \cdot D}{\mu} \quad (3.8)$$

$$P(z = 0, r) = P^{IN} \quad (3.9) \quad \text{B.C.}_{RI}$$

MODEL BUILDING AND VALIDATION

In equation 3.6 the overall heat transfer coefficient is mentioned. The formula to calculate it is the following:

$$Nu = \frac{U \cdot d_{PE}}{\lambda_g} = 1.26 \cdot Re_{d_{PE}} \cdot Pr^{\frac{1}{3}} \cdot \left(\left(\frac{1 - (1 - \phi)^{\frac{5}{3}}}{2 - 3 \cdot (1 - \phi)^{\frac{1}{3}} + 3 \cdot (1 - \phi)^{\frac{5}{3}} - 2 \cdot (1 - \phi)^2} \right) \cdot Re_{d_{PE}} \right)^{-\frac{2}{3}} \quad (3.10)$$

Equation 3.1 and 3.3 are balance equation. They follow the scheme:

$$Acc = In - Out + Prod$$

The former is respect to the number of moles present in the reactor. The accumulation of them is counteracted by the flux of moles going in and out from the unit adjust by the moles produced from the reactions.

The second is an energy balance where, with the assumption asserted in the beginning of this chapter, all the types of energy, except for the enthalpy, are neglected. These balances are coupled with the boundary conditions in both axial (3.2, 3.4) and radial (3.5, 3.6) coordinates.

In order to completely satisfy equation 3.6, the heat transfer coefficient has to be calculated by means of equation 3.10.

Equation 3.7 is the equation that allows for the calculation of the Pressure Drop inside the reactor and it is coupled with the boundary condition displayed by 3.9.

3.3.1 Kinetic scheme

To evaluate the reaction rate used in the aforementioned equations the model proposed by [43] was used. Eq. 1.5, 1.6 and 1.7 are the reaction that take place in the reactor and their reaction rate formulas are respectively:

$$r_1 = \frac{k_{ps1} \cdot K_{CO} \cdot f_{CO} \cdot f_{H_2}^{1.5} \cdot \left(1 - \frac{f_{CH_3OH}}{f_{CO} \cdot K_{eq,1} \cdot f_{H_2}^2}\right)}{(1 + K_{CO} f_{CO} + K_{CO_2} f_{CO_2}) \cdot (f_{H_2}^{0.5} + KK \cdot f_{H_2O})} \quad (3.11) \quad \left[\frac{mol}{s \cdot Kg_{CAT}}\right]$$

$$r_2 = \frac{k_{ps2} \cdot K_{CO_2} \cdot f_{CO_2} \cdot f_{H_2} \cdot \left(1 - \frac{f_{H_2O} \cdot f_{CO}}{K_{eq,2} \cdot f_{CO_2} \cdot f_{H_2}}\right)}{(1 + K_{CO} f_{CO} + K_{CO_2} f_{CO_2}) \cdot (f_{H_2}^{0.5} + KK \cdot f_{H_2O})} \quad (3.12) \quad \left[\frac{mol}{s \cdot Kg_{CAT}}\right]$$

$$r_3 = \frac{k_{ps3} \cdot K_{CO_2} \cdot f_{CO_2} \cdot f_{H_2}^{1.5} \cdot \left(1 - \frac{f_{CH_3OH} \cdot f_{H_2O}}{K_{eq,3} \cdot f_{CO_2} \cdot f_{H_2}^3}\right)}{(1 + K_{CO} f_{CO} + K_{CO_2} f_{CO_2}) \cdot (f_{H_2}^{0.5} + KK \cdot f_{H_2O})} \quad (3.13) \quad \left[\frac{mol}{s \cdot Kg_{CAT}}\right]$$

MODEL BUILDING AND VALIDATION

To calculate the f_i , the product between partial pressure and the fugacity coefficient (ϕ) has been calculated by means of the Redlich-Kwong-Soave (RKS) equation of state [44]. In the range of temperature of interest for our model, the equilibrium constant for equation 1.5 - 1.7 are:

$$K_{eq,1} = 10^{\left(\frac{5139}{T} - 12.61\right)} \quad (3.14)$$

$$K_{eq,2} = 10^{\left(\frac{-2073}{T} + 2.029\right)} \quad (3.15)$$

$$K_{eq,3} = K_{eq,1} \cdot K_{eq,2} \quad (3.16)$$

Due to the fact that the equation 1.7 is linearly dependent from equation 1.5 and 1.6, its equilibrium constant is just the product between the two equilibrium constants.

The kinetic parameters and the adsorption constants to calculate the reaction rate 3.10-3.12 are [45]:

$$k_{ps1} = 42.69 \cdot 10^7 \cdot e^{\left(-\frac{109900}{R \cdot T}\right)} \quad (3.17)$$

$$k_{ps2} = 7.31 \cdot 10^8 \cdot e^{\left(-\frac{123400}{R \cdot T}\right)} \quad (3.18)$$

$$k_{ps3} = 4.36 \cdot 10^2 \cdot e^{\left(-\frac{65200}{R \cdot T}\right)} \quad (3.19)$$

$$k_{CO} = 7.99 \cdot 10^{-7} \cdot e^{\left(\frac{58100}{R \cdot T}\right)} \quad (3.20)$$

$$k_{CO2} = 1.02 \cdot 10^{-7} \cdot e^{\left(\frac{67400}{R \cdot T}\right)} \quad (3.21)$$

$$KK = 4.13 \cdot 10^{-1} \cdot e^{\left(\frac{104500}{R \cdot T}\right)} \quad (3.22)$$

Considering that each catalyst can have a different activity depending on the supplier, a value of 1.9 has been multiplied to the reaction rates in order to reach an accordance between the experimental and the calculated value of Temperature inside the reactor [7].

The catalyst used is CuO/ZnO/Al₂O₃ due to the high thermal conductivity brought from the copper substrate.

3.4 Separation and recycle section

MODEL BUILDING AND VALIDATION

The separation section consists on a cooler, to cool down the product stream to 37°C as seen in [46] and an ideal flash, indicated as component splitter in Aspen HYSYS, with which methanol and water are sent on the liquid stream while all the other compounds on the vapor one. After these two units a splitter, to allow for a small purge avoiding accumulation and too high flowrate is added. The purge ratio is changed so that the inerts mole fraction at the reaction inlet is kept to 8.82%. At the end the recycle operator to allow for the recycling of reactants is inserted. The numerical method used is the forward Wegstein method with 1000 as maximum number of iterations. Table 3.3 shows all the sensitivity used to reach the convergence for the properties of the flow.

	Sensitivities	Unit
Vapor Fraction	0.1	[-]
Temperature	0.1	[K]
Pressure	0.1	[bar]
Flow	0.1	[kmol/h]
Enthalpy	0.1	[J/mol]
Composition	0.001	[-]
Entropy	0.1	[J/mol K]

Table 3.3 Recycle parameters

3.4 Model Validation

To validate the model, it is useful to understand whether or not the temperature and pressure profiles correspond to the ones proposed by [7]. In both the graphs of Figure 3.3 and 3.4, the temperature profile can be divided in three phases:

- The first phase until $z^\circ < 0.15$ (which means $z < 1.2$ m), in which the T_{cool} is higher than T , thus the coolant is actually heating the process stream and the reactions didn't start yet.
- The second phase, where $0.15 < z^\circ < 0.25$ (which means $1.2 \text{ m} < z < 2$ m), in which the reactions start and the T reaches the maximum value.

MODEL BUILDING AND VALIDATION

During this phase, the coolant is contributing taking away the heat released from the exothermicity of the reactions.

- The last phase, until the reactor full length is completed, in which also the reverse reaction is taking place. The latter, due to their endothermicity, with the contribution of the coolant, are forcing the temperature decrease. A final plateau is almost reached, meaning that the process flow is approaching the thermodynamic equilibrium. Considering that the outlet temperature is higher than the coolant one, the equilibrium is not completely obtained. To further validate this statement a simulation with a tool in Aspen HYSYS called Gibbs reactor has been done. This tool allows to simulate a reactor whose reactions are at the equilibrium. Fixing all the parameters as in the previous simulations, the results are displayed in table 3.4. The Gibbs reactor does not allow for a temperature profile inside the reactor, being it a column with a fixed reaction set already present in Aspen library, but from the results shown in Table 3.4 it is clearly understandable that its performances are slightly better than the model ones.

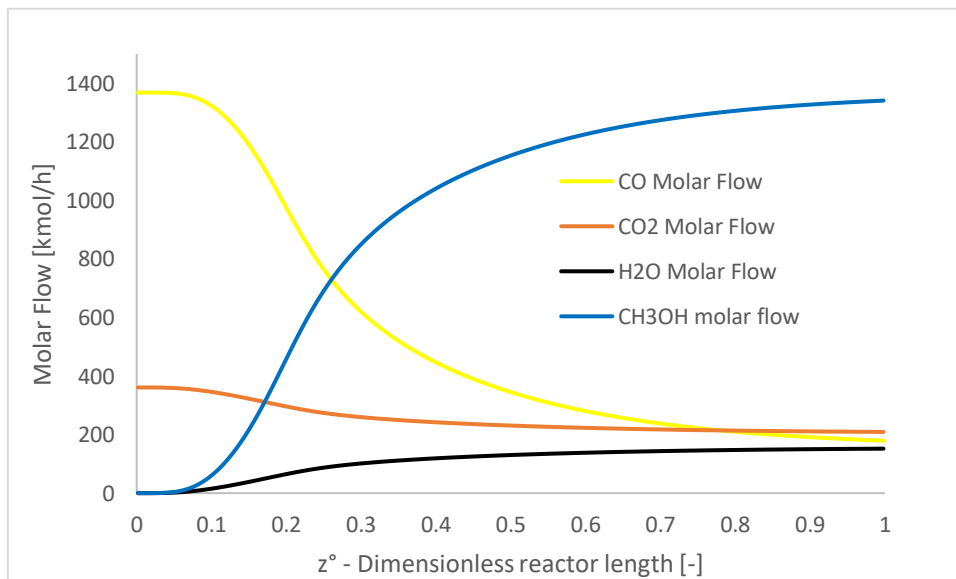


Figure 3.2 Molar flows inside the reactor.

The three phases above mentioned are also recognisable from Figure 3.2. Initially, a small amount of methanol and water is produced and a small amount of CO and CO₂ is used to fulfil this purpose. Entering the second phase (when z° > 0.15) the amount of product increases while the reactants concentration starts

MODEL BUILDING AND VALIDATION

to fall down. At the end, the plateau is clearly visible, due to the approaching to the thermodynamic equilibrium between the components of the mixture.

Regarding the Pressure profile, it is a linear decrease due to the pressure drops inside the reactors. Values of this parameters are not so high and they will be regained with the recompression before the recycle. The small difference found between the model and [7] are due to the assumptions made in the beginning of this chapter.

MODEL BUILDING AND VALIDATION

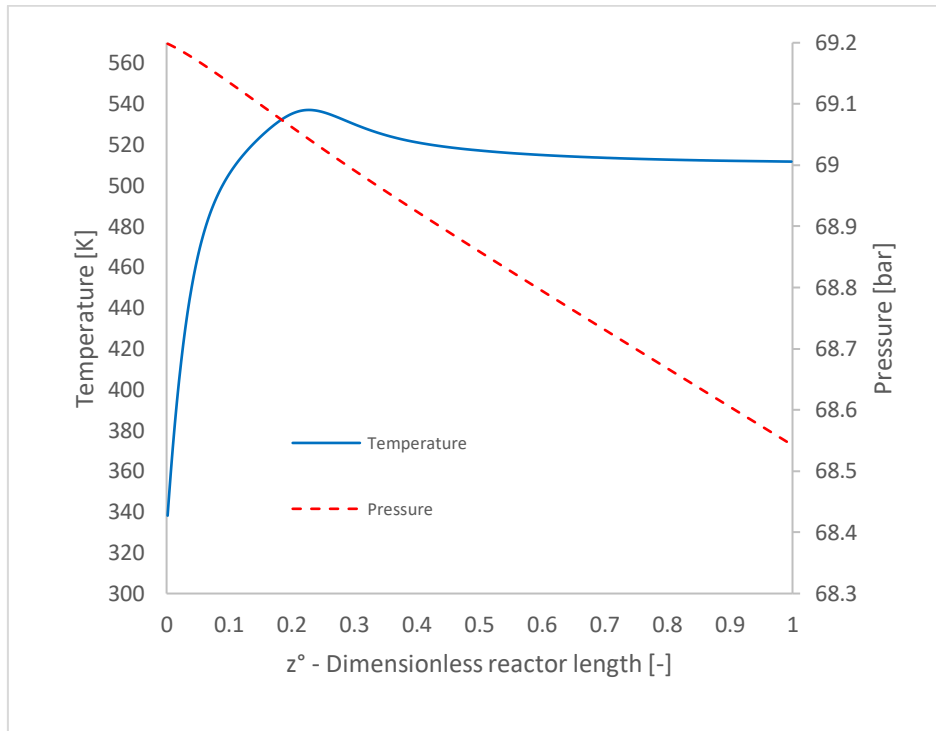


Figure 3.3 Temperature and Pressure profile at centerline vs reactor length. Blue solid line: Temperature, red dashed line: Pressure.

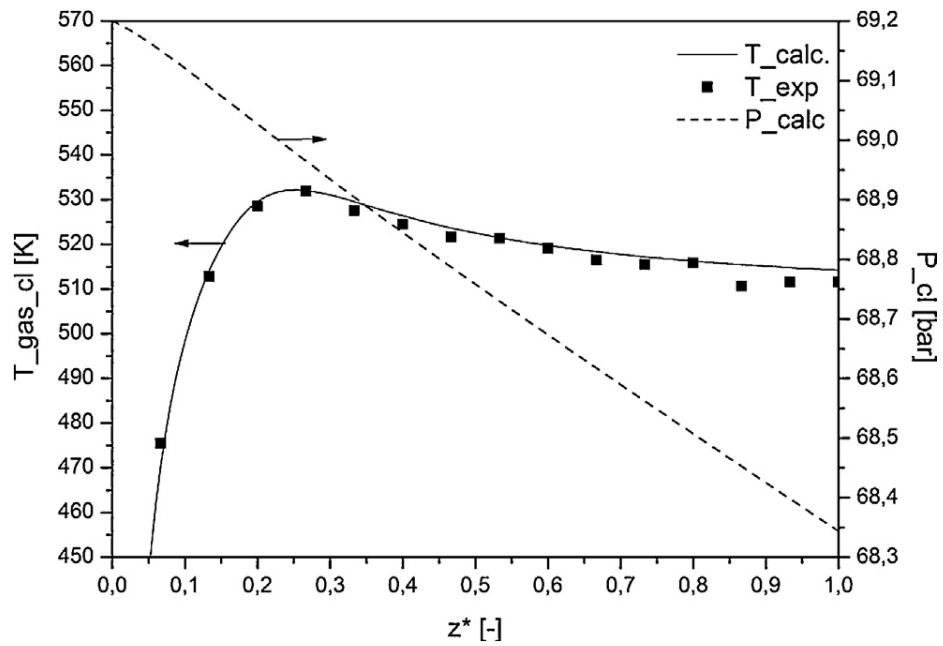


Figure 3.4 Temperature and Pressure profile from Montebelli et al. [7].

MODEL BUILDING AND VALIDATION

Furthermore, looking at Table 3.4 the results obtained by [7] and this model are pretty similar. The CO_x conversion, the MeOH Productivity and the RR are slightly higher in the model proposed by [7]. Taking into account the assumption made at the beginning in this chapter, the differences are acceptable.

The H₂ is in excess, an unavoidable accumulation of it will be noticed. If the reaction extent calculated in this model is lower, pointed out by of the lower CO_x reacted, the hydrogen accumulation will increase, justifying the aforementioned differences and also the higher M_I.

At the end, comparing the hotspot temperatures, the one proposed by [7] is lower, implying a better heat exchange with the coolant as displayed by the U value.

	[7] Montebelli et al.	Model	Equilibrium Model
CO _x Conversion χ %	78.6	77.5	79.73
MeOH Productivity [ton/day]	1112	1031	1070
RR	3.26	3.14	2.985
M _I	8.13	8.28	8.212
T _{HotSpot}	534	537	/
U [W/m ² K]	900	810	/

Table 3.4 PB reactor material balance: calculated vs Montebelli et al. values.

3.6 Separation section with flash

As mentioned on the precedent paragraph, the work done by [7] rely on a separation section that consists on an ideal situation in which methanol and water are completely separated in the liquid phase. In a real case this will not be achieved so easily, because also a small percentage of methanol will be present in the vapor. This phenomenon will lead to recirculation of methanol, leading to an increase in the reaction rate of the reverse reactions and an actual loss in performances.

MODEL BUILDING AND VALIDATION

	[7] Montebelli et al.	Improved Model
CO _x Conversion χ %	78.6	87.12
MeOH Productivity [ton/day]	1112	271.37
MeOH Productivity / Fresh Feed [-]	Unknown	0.3083
RR	3.26	14.75
M _i	8.13	39.32
T _{HotSpot}	534	518.15

Table 3.5 PB reactor material balance: Montebelli et al. [7] vs improved model.

Even though the conversion of CO_x increases a lot, their concentration defect (Figure 3.6), compared to the H₂ one, is so exaggerated that the methanol produced will be in a very low quantity. The H₂ that will remain as excess in the loop will be recycled back at every iteration, leading to an accentuation of this irregularity. This is why the RR and the M_i increase as well (Table 3.5). The number that correspond to Methanol productivity /Fresh Feed (Normalized Methanol Productivity) is not present in [7] to be compared, but it will result useful to compare the next simulations that have been implemented.

It can be said that in this case the reactor inlet is so diluted by the H₂, that almost all the CO_x present are converted into methanol since they are the limiting agent. Consequence of this is that the temperature profile reaches a maximum that is lower than the one before calculated as shown in Figure 3.3.

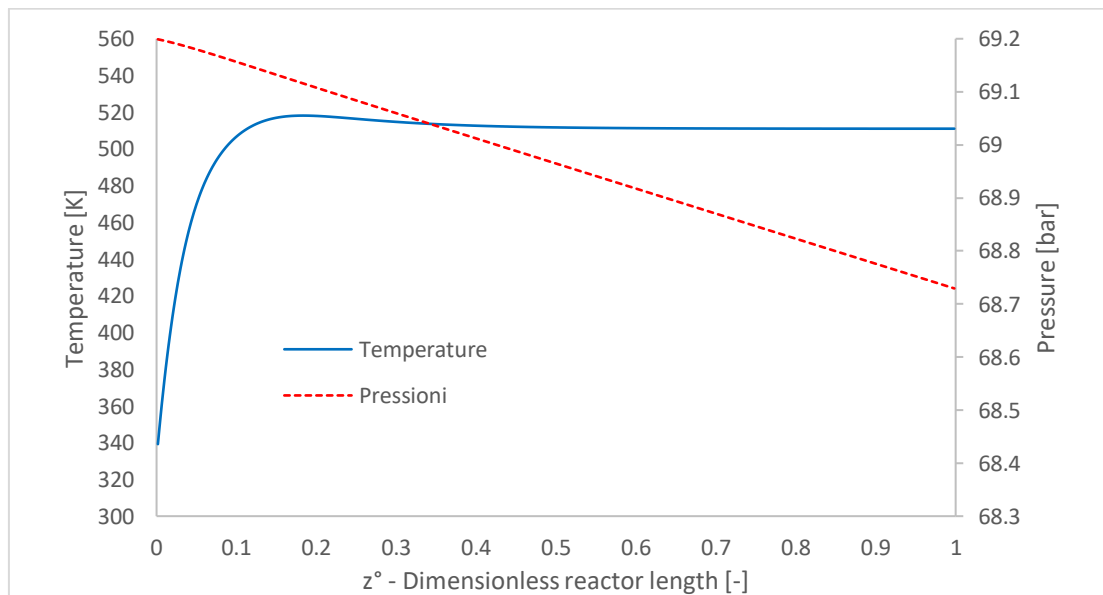


Figure 3.5 Temperature and Pressure profile at centerline vs reactor length for the improved model. Blue solid line: Temperature, red dashed line: Pressure.

MODEL BUILDING AND VALIDATION

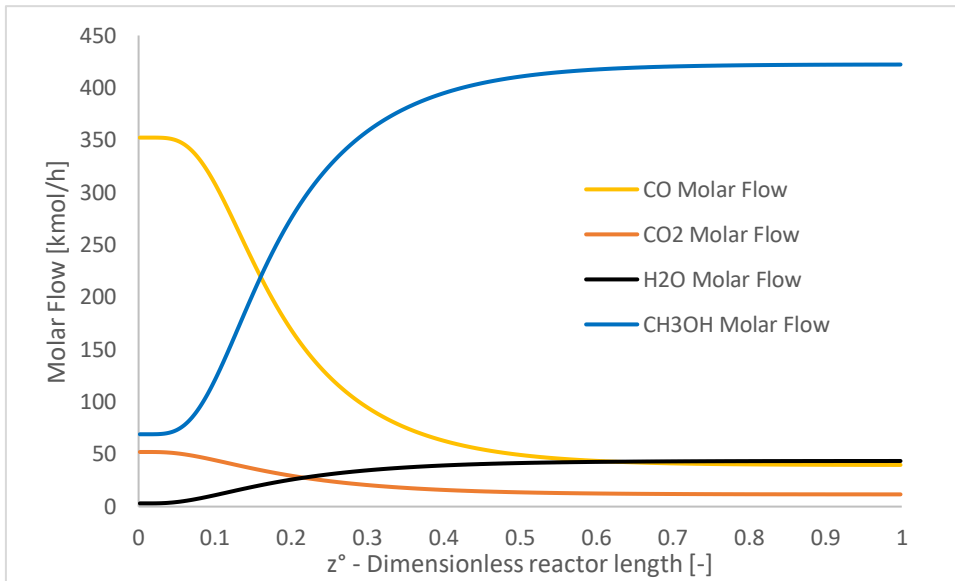


Figure 3.6 Molar flows inside the reactor for the improved model.

Figure 3.6 shows the same trend as Figure 3.2. The only difference are the values, lower for the former. An important discrepancy that has to be enhanced is that, for the improved model, also methanol and a bit of water are present at the reactor inlet, cause of the decreased productivity.

MODEL BUILDING AND VALIDATION

4

Different cases simulations

The aim of this chapter is to apply the model developed in the precedent one, to other fresh feed composition coming from the gasification of biomasses. The particularity of these new simulations is that the M_I is no longer in the optimal range, meaning that the productivity of methanol has to be optimized. To do so, the temperatures inside the reactor have been changed (both T_{IN} and T_{cool}) and a numerical simulation considering the addition of pure H_2 to reach the optimal stoichiometric coefficient has been carried out. Also, a new different technology involving two fixed bed reactors in series (Lurgi configuration) to better follow the optimal methanol conversion curve displayed in Figure 1.7 has been simulated.

4.1 Identification of the new inlet stream

In this section the streams on which the simulation will be carried out are displayed. The aim is to maximize the performances of the reactor trying to allow the production of methanol also from fresh feed that do not present an excess of H_2 .

EVALUATION OF THE CASES

Stream 2E	Value
y_{CO} [-]	0.323
y_{CO_2} [-]	0.025
y_{H_2O} [-]	0.0
y_{H_2} [-]	0.648
y_{CH_4} [-]	0.001
$y_{C_2/C_3/C_4+}$ [-]	0.0
y_{N_2} [-]	0.003
FF [kmol/h]	828.6
M_F [-]	1.790

Table 4.1 Properties of a stream coming from the reforming+ CO₂ capture of bio-NG.

Stream 2D, shown in Table 4.2, is a dry stream, coming from the Reforming of bio-natural gas with a subsequent capture of the CO₂. Its stoichiometric modulus is near the optimal one but still lower.

Stream 2D	Value
y_{CO} [-]	0.224
y_{CO_2} [-]	0.323
y_{H_2O} [-]	0.0
y_{H_2} [-]	0.45
y_{CH_4} [-]	0.001
$y_{C_2/C_3/C_4+}$ [-]	0.0
y_{N_2} [-]	0.002
FF [kmol/h]	1160
M_F [-]	0.232

Table 4.2 Properties of a streaming coming from the reforming of bio-NG.

EVALUATION OF THE CASES

Stream 2D, shown in Table 4.2, is a dry stream coming from the reforming of Bio-natural gas, without capturing the CO₂. Its modulus is very low, leading to a different set of parameters in order to achieve a satisfying methanol production.

4.2 Stream 2E simulation

In this paragraph, all the simulation based on the stream coming from the reforming + CO₂ capture of bio-NG are presented. The final aim is to optimize the methanol productivity, without losing touch with other variables, such as hotspot temperature, RR and inerts content, that can actually influence an economical profitability of the investment for the plant.

4.2.1 Constant N_T

The simulation loop is the same as the one shown in Figure 3.1. keeping constant all the parameters of the initial model based on [7]. The only thing that changes is the Fresh Feed composition and molar flow.

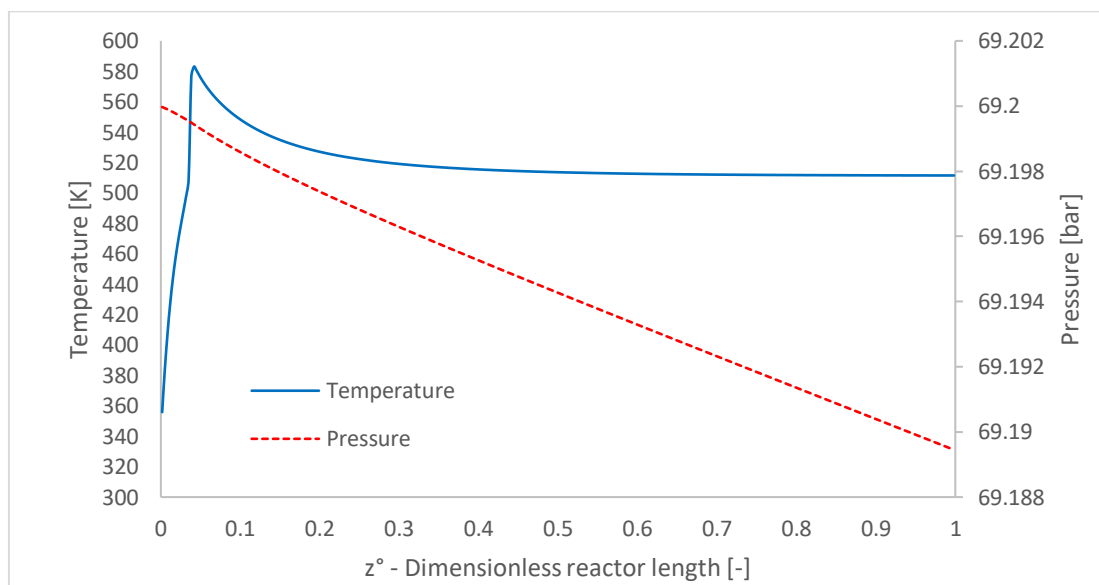


Figure 4.1 Temperature and Pressure profile at centerline vs reactor length for stream 2E with constant $N_T = 4650$. Blue solid line: Temperature, red dashed line: Pressure.

As Figure 4.1 shows, the temperature profile reaches a maximum at a very early stages of the reactor, meaning that the reactions start quickly. The main problem is the value of the maximum temperature reached. A $T_{\text{HotSpot}} \approx 580$ K is so high that is dangerous not only for the side reactions but also for the resistance of the catalyst to these values of temperature. This configuration is not practicable in a

EVALUATION OF THE CASES

real life plant thus some changes has to be implemented. For this reason, it makes no sense to look at the performances results.

Increasing the inerts content

If the inerts content in the reaction loop is increased, the phenomenon of diluting the stream and absorbing the heat of reaction will actually help in containing the T_{HotSpot} . The flow ratio set in the splitter for the simulation in the previous paragraph was 0.989, meaning that 98.9% of the vapor stream coming out from the flash is recycled back. Increasing this ratio to 0.9995 the inerts content in the reactor inlet inevitably increases.

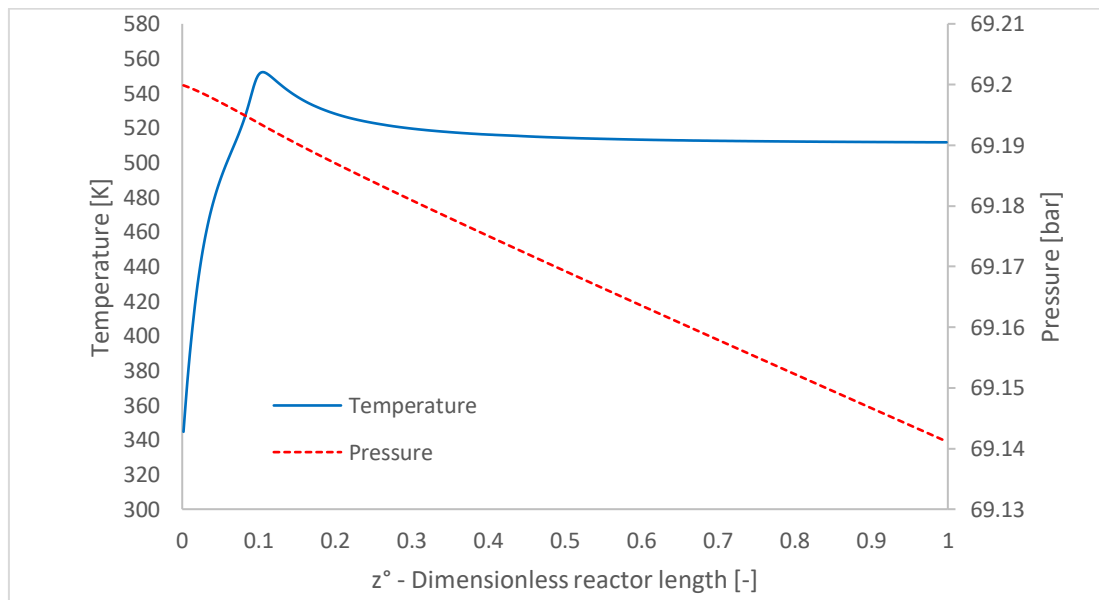


Figure 4.2 Temperature and Pressure profile at centerline vs reactor length for stream 2E with constant $N_T = 4650$ and flow ratio = 0.9995. Blue solid line: Temperature, red dashed line: Pressure.

From Figure 4.2 it's clear that T_{HotSpot} decreased to 550 K, value that could be acceptable but still a bit higher and can lead to methanation reaction (loss in selectivity and unstable system). Even though this simulation can be applicable, the inerts content in the reactor inlet increases a lot, reaching value of 20 %.

Table 4.3 shows the useful parameters to understand whether or not the configuration is profitable if applied to a real life plant. The number are very promising but still, the problem regarding the temperature can't be neglected.

EVALUATION OF THE CASES

	Stream 2E with high inerts content in the RI
CO _x Conversion χ %	20.41
MeOH Productivity [kmol/h]	267.46
Normalized CH ₃ OH Prod. [-]	0.3228
RR [-]	2.47
M _i [-]	0.4521
RI [kmol/h]	2876

Table 4.3 Performances of the reactor with as fresh feed stream 2E and higher flow ratio in the splitter.

4.2.2 Constant Reactor Inlet / N_T

In this configuration, what has been fixed is the ratio between the RI flow rate and the N_T in a way that the molar flow per tube is constant. The number found in the model presented by [7] is 3.877 [kmol/h] per each tube and this will be the goal. To do so, the number of tubes will be optimized, reaching a value of 633 tubes.

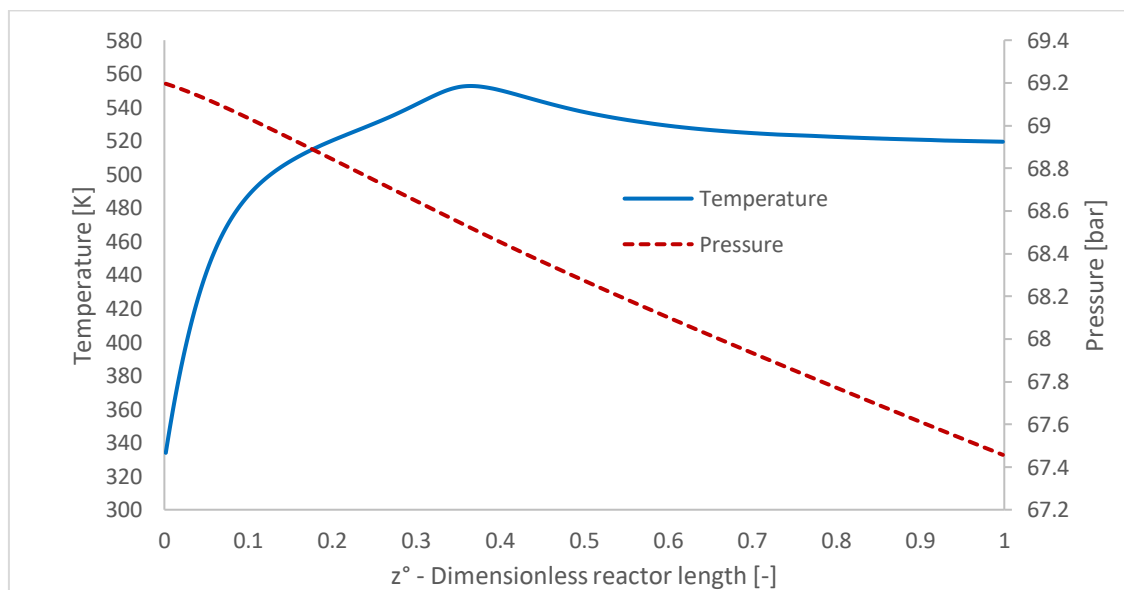


Figure 4.3 Temperature and Pressure profile at centerline vs reactor length for stream 2E with constant $RI/N_T = 3.877$ kmol/h per each tube. Blue solid line: Temperature, red dashed line: Pressure.

As it can be noticed from Figure 4.3, $T_{HotSpot}$ is still too high, leading to already mentioned issues. Considering the performances in Table 4.4, it could be useful to further investigate in this line of simulation.

EVALUATION OF THE CASES

	Stream 2E Flow rate per tube constant
CO _x Conversion χ %	24.41
MeOH Productivity [kmol/h]	263.63
Normalized CH ₃ OH Prod. [-]	0.31817
RR [-]	1.8839
M _i [-]	0.8251
RI [kmol/h]	2390

Table 4.4 Performances of the reactor with stream 2E as fresh feed and $RI/N_T = 3.877$ kmol/h per each tube.

Decreasing T_{cool}

Seen that the previous simulation resulted on a too hot reactor, leading to troubles regarding selectivity and catalyst activity, the next step is decreasing the T_{cool} in order to reach an acceptable value of $T_{HotSpot}$. The latter has been set to 538 K, value for which almost no methanation will occur [47] and no runaway could happen.

Also in this case, an optimization of the ratio between the RI flow rate over the N_T has been implemented, meaning that a two variable (T_{cool} and N_T) optimization is needed. To reach the same value of the ratio found by [7] (3.877 [kmol/h] per each tube), 708 tubes are necessary.

The value for T_{cool} found in this chapter is 507.15 K.

Lower temperatures cause a too small heat exchange in the first part of the reactor, leading to the non-activation of the reactions. Thus, the temperature profile in this simulation resulted on a flat line. As consequence, nothing occurred in the reactor and to reach the convergence, the quantity of the flow recycled increased at each iteration. This phenomenon continues until a maximum value of pressure-drops inside the reactor for which the simulation stops automatically.

Higher temperatures, as mentioned in the previous simulations presented, cause a $T_{HotSpot}$ that is too high causing loss in selectivity and safety.

The temperature profile found and displayed in Figure 4.4 is pretty similar to the one in Figure 4.3. The maximum value of temperature is shifted to the right and is lower as expected. This is due to the lower initial heat exchanged between cooler (heating behaviour) and process stream. Consequence of this, is also that the outlet temperature of the mixture exiting the reactor is lower.

Of course, decreasing the $T_{HotSpot}$ and shifting to the right its reached (the second part mentioned in paragraph 3.5) means that the reactions will have less reactor

EVALUATION OF THE CASES

length to occur and the performances will decrease. Table 4.5 shows that methanol productivity goes down but not in an excessive quantity.

This configuration is the first configuration acceptable in terms of safety and will be the base to understand whether or not next ones are better.

	Stream 2E Flow rate per tube constant with $T_{cool} = 507.15$ K
CO _x Conversion χ %	20.48
MeOH Productivity [kmol/h]	262.50
Normalized CH ₃ OH Prod. [-]	0.3168
RR [-]	2.2978
M _i [-]	0.7694
RI [kmol/h]	2732

Table 4.5 Performances of the reactor with stream 2E as fresh feed, $RI/N_T = 3.877$ kmol/h per each tube and $T_{cool} = 507.15$ K.

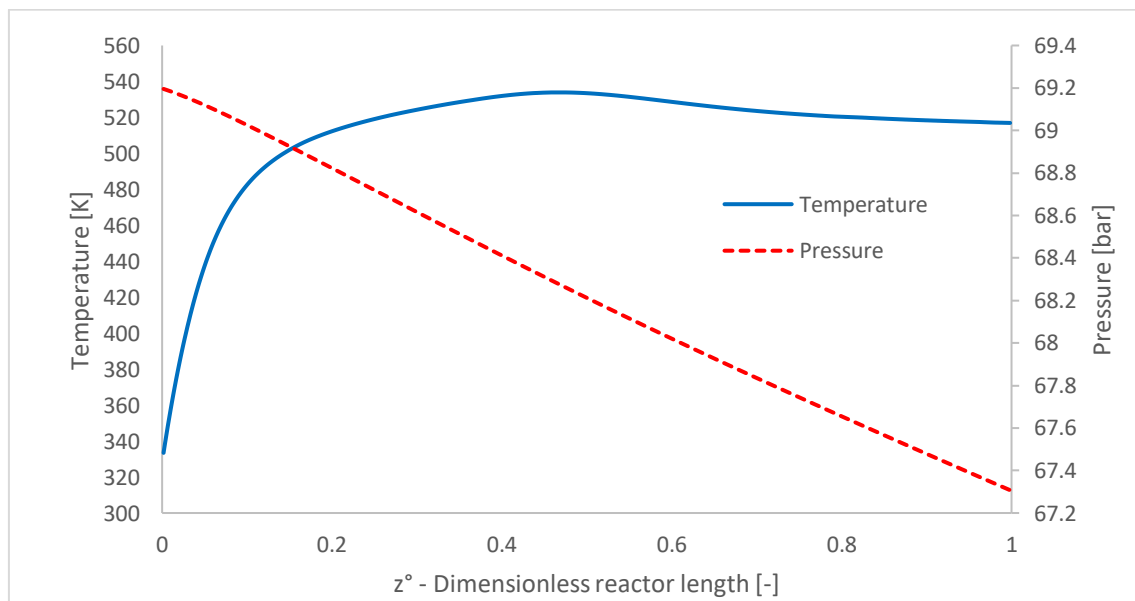


Figure 4.4 Temperature and Pressure profile at centerline vs reactor length for stream 2E with constant $RI/N_T = 3.877$ kmol/h per each tube and T_{cool} decrease to 507.15 K. Blue solid line: Temperature, red dashed line: Pressure.

EVALUATION OF THE CASES

Changing T_{IN}

In the precedent paragraph, the simulation implemented was a good one in terms of $T_{HotSpot}$ but the performances were questionable. The main doubt was that the first part of the reactor was actually used to bring the reactants to T_{React} and was in some way wasted part of the catalyst mass for this purpose. Trying to improve the model, as in the work done by [48, 49], what it can be changed is the inlet temperature of the mixture, leading to an effective usage of the whole catalyst length to allow the progress of the reactions. Increasing the T_{IN} of course lead to a hotter reactor and would need a decreasing in the T_{cool} in order to maintain safe the loop. A hypothesis considered here is that T_{IN} should not exceed T_{cool} , coupled with the $T_{HotSpot}$ value set to 534 K as before. The N_T remains the same value of the precedent simulation (708) and the ratio value used in the splitter as well (0.9930).

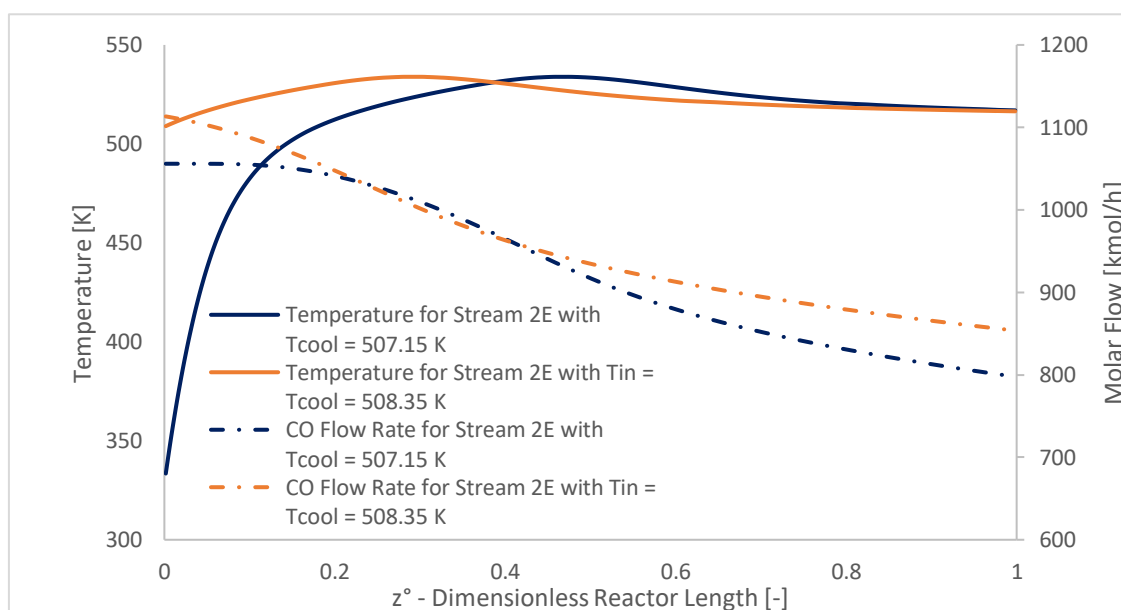


Figure 4.5 Temperature and CO molar flow for simulation with as fresh feed stream 2E. Blue line: $T_{cool} = 507.15$ K and $T_{in} = 323$ K; Orange line: $T_{in} = T_{cool} = 508.35$ K; Continue line: Temperature [K]; Dashed line: CO molar Flow [kmol/h].

EVALUATION OF THE CASES

In Figure 4.5 are shown both temperature and CO molar flow profile for the simulation of the stream 2E with $T_{cool} = 507.15$ K and $T_{IN} = 323$ K and the simulation of the stream 2E with $T_{cool} = T_{IN} = 508.35$ K. Looking at the CO molar flow some phases it can be seen:

- In the first part of the graph, the CO rate of consumption of the simulation in which $T_{IN} = 508.35$, is higher than the other simulation. This is due to the fact that the reactions start already at the beginning of the reactor instead, for the simulation starting from a lower temperature, this part is actually used to heat the reactants.
- In the second part of the graph, the CO rate of consumption is higher for the simulation with $T_{IN} = 323$ K. The explanation of this phenomenon is quite complicated: if we look at the mixture composition at $z^o = 0.5$ (where the blue line reaches the THotSpot) there will be more methanol in the simulation started from a higher temperature than the other one. The presence of methanol will inhibit the direct reaction and enhance the inverse reaction, leading to a decreased overall reaction rate.

In other words, the “blue simulation” will not use the first part of the reactor, while the other will not only not use the last part but will use it to re-create reactants. These hypotheses are also verified by the reactor performances displayed in Table 4.6. Even though the methanol productivity increases to 264.02 kmol/h compared to the 262.50 kmol/h, the other parameters point out the weaknesses before mentioned with a smaller CO_x Conversion and higher RR.

	Stream 2E Flow rate per tube constant with $T_{IN} = T_{cool} =$ 508.35 K
CO_x Conversion χ %	19.33
MeOH Productivity [kmol/h]	264.02
Normalized CH ₃ OH Prod. [-]	0.3186
RR [-]	2.418
M_i [-]	0.6691
RI [kmol/h]	2832

Table 4.6 Performances for a reactor with stream 2E as fresh feed and $T_{IN} = T_{cool} = 508.35$ K.

This last sentence leaves some doubt about if 508.35 K is the optimum temperature to set as T_{IN} and T_{cool} . To be completely sure about this, some simulation changing in a small range $T_{IN} = T_{cool}$ have been carried out.

EVALUATION OF THE CASES

	Stream 2E Flow rate per tube constant with $T_{IN} = T_{cool} = 508.15$ K	Stream 2E Flow rate per tube constant with $T_{IN} = T_{cool} = 508.55$ K
CO _x Conversion χ %	7.8975	21.36
MeOH Productivity [kmol/h]	255.69	264.4
Normalized CH ₃ OH Prod. [-]	0.3086	0.3191
RR [-]	6.787	2.17
M _i [-]	0.6375	0.7018
RI [kmol/h]	6093	2626

Table 4.7 Performances for a reactor with stream 2E as fresh feed and 1) $T_{IN} = T_{cool} = 508.15$ K; 2) $T_{IN} = T_{cool} = 508.55$ K.

Simulating the same stream 2E with $T_{IN} - 0.2$ K and $T_{IN} + 0.2$ K (Table 4.7) it can be seen that the former leads to worse results, caused by the very bad reaction rates in the last part of the reactor and the not that good performances in the first part, while for the latter, in which the temperature is increased, the outcomes are better. Of course, the THotSpot is higher (538 K compared to 534 K) but still is in the range of safe operations. This is proven by the temperature profiles in Figure 4.6. The red line, the optimal one, reaches a higher maximum value, but it however reaches the “plateau” before the others, leading to a faster approach to the thermodynamic equilibrium.

Simulation with really higher or lower $T_{IN} = T_{cool}$ can't be accomplished because of the too hot/cold reactor leading to problems already presented.

EVALUATION OF THE CASES

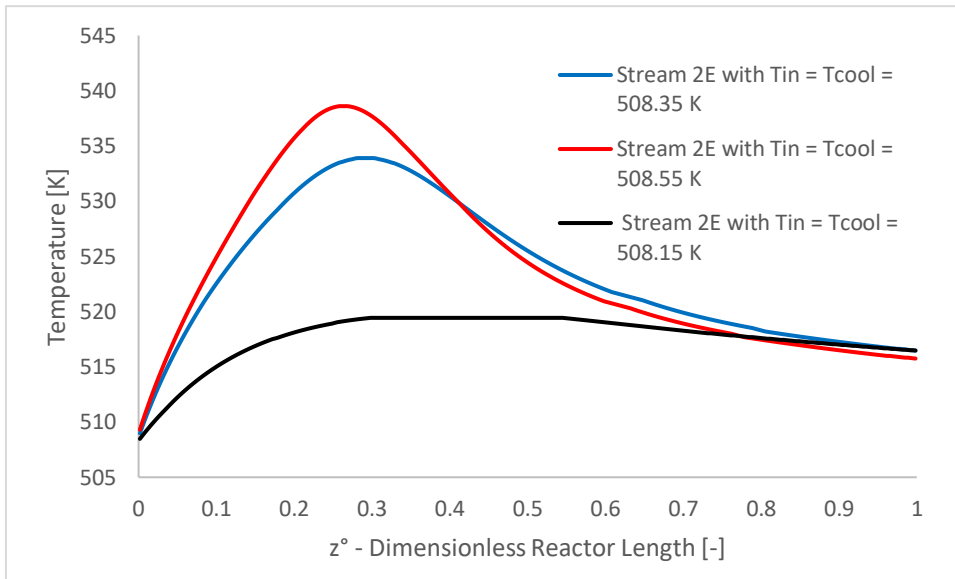


Figure 4.6 Temperature profile at centerline vs reactor length for stream 2E with $N_T = 708$. Blue solid line: $T_{IN} = T_{cool} = 508.35$ K, Red solid line: $T_{IN} = T_{cool} = 508.55$ K, Black solid line: $T_{IN} = T_{cool} = 508.15$ K.

4.2.3 Adding H₂

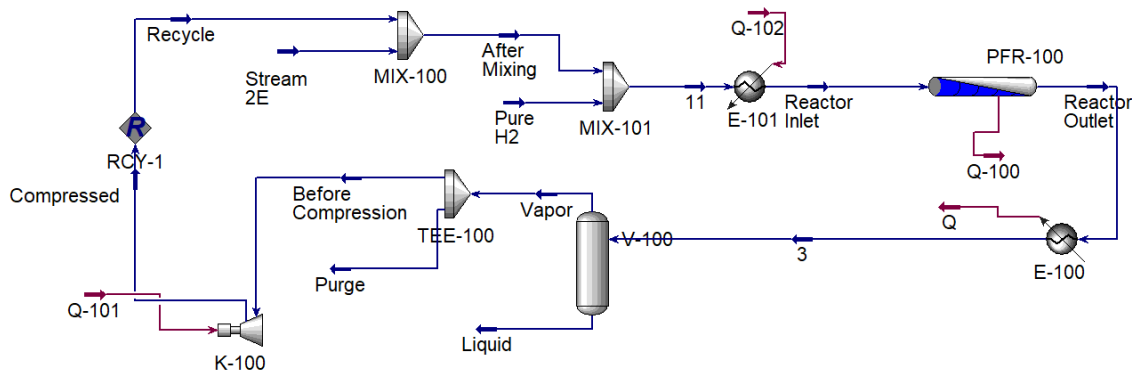


Figure 4.7 Synthesis loop when a pure H₂ stream is added to the fresh feed mixed with the recycle.

From the precedent simulation, it has been outlined that the main weak point is the M_I not in the range of the optimal one. A pure H₂ stream can be added to the old reactor inlet stream, in a way that the M_I value increases and the performances are improved. Figure 4.7 shows the synthesis loop used. After the first mixer, a second one where the stream “After mixing” and the stream “Pure H₂” are mixed together to create the new reactor inlet, that then is heated up to the level of temperature desired. Of course, it is not known how much H₂ has to be added in order to optimize the important parameters. To find that value, a series of simulation changing the H₂ quantity have been implemented. N_T (708), flow ratios value in the splitter (0.9930) and $T_{HotSpot}$ (534 K) are considered fixed at their previously found value in order to compare the results found.

EVALUATION OF THE CASES

Figure 4.8 shows the temperature profile of all the simulation implemented. The higher is the quantity of H₂ added to the stream “After mixing”, the sooner the T_{HotSpot} will be reached. Looking at the temperature behaviour the simulations that involve from 20 to 65 kmol/h of H₂ added are the best one in terms of approaching the thermodynamic equilibrium. The plateau is almost reached and the T_{cool} as well, meaning that the rates of reaction are advancing toward the zero value. Moreover, if we look at Table 4.8, even though the CO_x conversion is higher if more H₂ is added (this is obvious since the excess of H₂ becomes more and more prominent), RR and Normalized Methanol Productivity (the one that include the H₂ stream) are more interesting in the initial cases. Just thinking roughly about costs, the lower is the RR, the less expensive will be the recompression of the streams and the lower is the H₂ needed, the lower are the cost related to its production/purchase.

	H ₂ added [kmol/h]	RR [-]	M _I [-]	CO _x Conversion χ %	MeOH Productivity [kmol/h]	Normalized CH ₃ OH Prod. Over Fresh Feed [-]	Normalized CH ₃ OH Prod. Over Fresh Feed + H ₂ [-]	RI molar flow (adding H ₂) [kmol/h]	T _{IN} = T _{cool}
1	20	1.502	1.625	42.04	272.32	0.3287	0.3209	2074 (2094)	501.05
2	35	1.571	2.486	54.40	277.20	0.3345	0.3210	2128 (2163)	500.65
3	50	1.872	3.741	65.77	281.60	0.3398	0.3205	2380 (2430)	502.05
4	65	2.660	6.253	75.95	285.17	0.3441	0.3191	3033 (3098)	505.75
5	70	3.128	7.492	78.14	285.95	0.3451	0.3182	3421 (3491)	507.75
6	75	3.715	8.963	79.73	286.44	0.3457	0.3170	3906 (3981)	509.95
7	80	4.395	10.60	80.38	286.85	0.3462	0.3157	4471 (4551)	512.15
8	85	5.148	12.35	80.74	287.03	0.3464	0.3142	5094 (5179)	514.15
9	90	5.944	14.09	80.29	287.09	0.3465	0.3125	5754 (5844)	516.05
10	95	6.755	15.91	80.11	287.25	0.3466	0.3110	6426 (6521)	517.45

Table 4.8 Performances for a reactor with as fresh feed stream 2E when different quantities of pure H₂ are added.

EVALUATION OF THE CASES

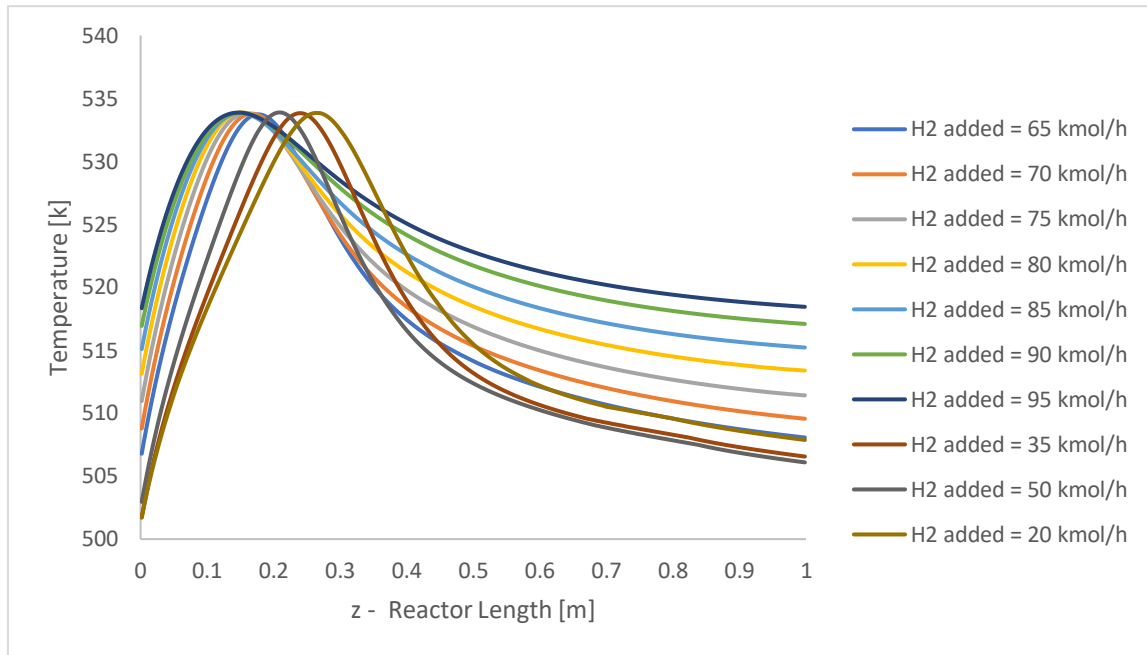


Figure 4.8 Temperature profile for a reactor with as fresh feed stream 2E and the addition of pure H₂ after the mixing with the recycle.

EVALUATION OF THE CASES

4.2.4 Lurgi Configuration

Another way to optimize the methanol production is to try to reach the thermodynamic equilibrium utilizing two reactors in series [50]. The benefit of this technology is to have low production cost at the maximum capacity. Thanks to the heat integration performed by the two reactors and thanks to the low recycle ratio in the synthesis loop, this technology is very interesting in the methanol scenario [51,52].

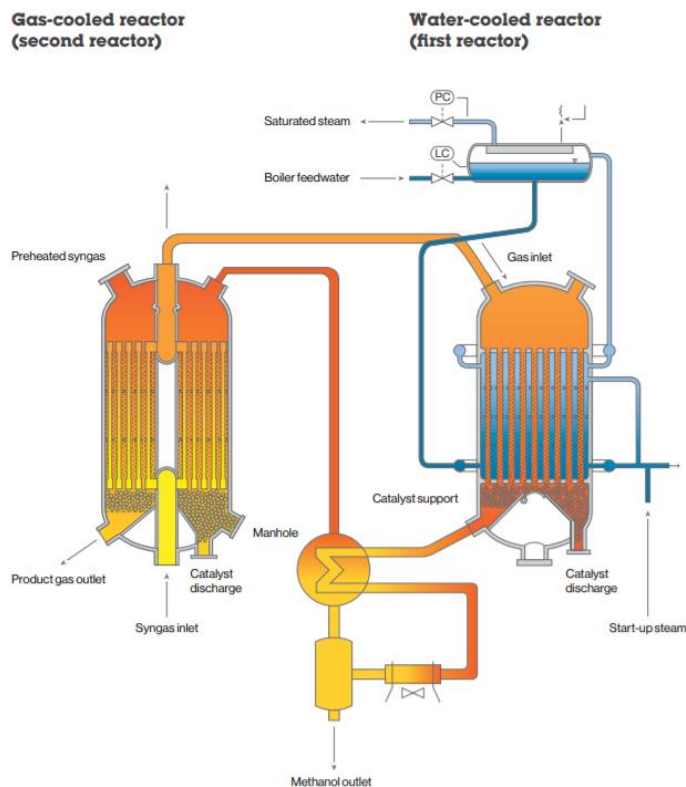


Figure 4.9 Lurgi configuration about methanol synthesis [53].

Figure 4.9 shows the configuration adopted: the syngas, already hot, pass through a first reactor tube side in which reacts on a catalyst support. Shell side of this reactor is a normal coolant like cooling water. The outlet stream of the first reactor goes through a second reactor, tube side on a catalyst support, in which the coolant is the initial cold syngas that will be preheated and sent to the inlet of the first reactor as above mentioned [54]. The temperature profile of the first reactor should be equal to the other temperature profiles shown in this chapter, while for the second reactor, the temperature, after a small increase, should decrease due to the exchange with the cold syngas. Decreasing the temperature of the second reactor, allows for a further approximation to the equilibrium curve.

EVALUATION OF THE CASES

What is important in this configuration is the inlet temperature of the first reactor. From this value, not only depends the temperature behaviour of the latter, but also the heat exchanged in the second reactor, thus the extent of reaction. Optimizing this temperature could help in the minimization of production and heat integration costs [55,56].

The main advantages of using two separates reactors are:

1° Reactor	2° Reactor
Reaction Control	Operate at optimum route
Quasi isothermal operation	Equilibrium driving force
High yield to methanol	High conversion of CO _x
High Energy efficiency	Substitute reactor preheater
Heat recovery to steam	Elimination of catalyst poisoning
Kinetic control	Thermodynamically control

Mixed together these advantages bring to the synthesis loop [57]:

- High overall syngas conversion
- Longer catalyst lifetime
- High capacity
- Lower investment costs

EVALUATION OF THE CASES

Aspen HYSYS simulation

Since in Aspen HYSYS V8.8 there is no unit operation that allows to design a tubular heat exchanger with reactions inside (just a PFR with tubes and catalyst in which a not simulated coolant is possible), some tricks have to be implemented to make this configuration allowable.

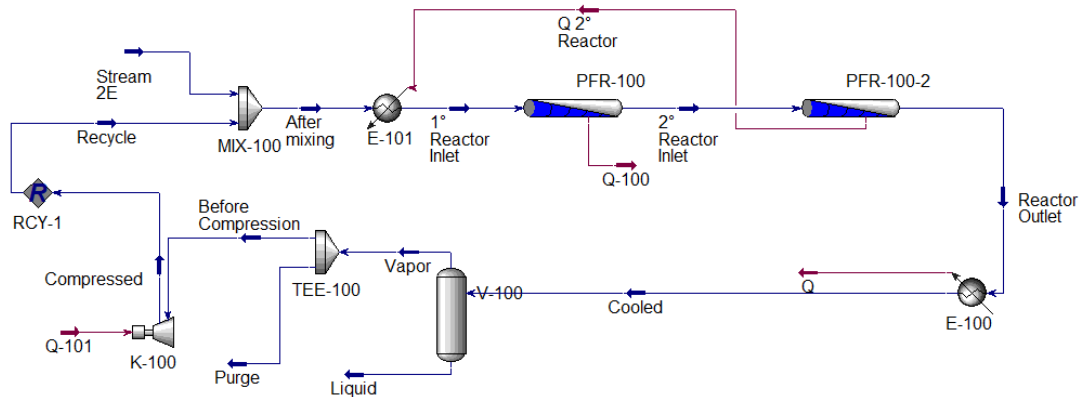


Figure 4.10 Lurgi Methanol synthesis loop in Aspen HYSYS V 8.8.

Figure 4.10 shows the loop used in Aspen HYSYS. After mixing the fresh feed and the recycle coming from the flash, a first heat exchange is performed. The heat flow used to preheat the first reactor inlet is connected to the second reactor, meaning that the energy is generated from cooling the stream passing through the second reactor. The previously mentioned energy is then used to preheat the first reactor inlet. With this trick the correlation between the two reactor is preserved, even though a heater is needed in the process loop.

As mentioned in the beginning of this paragraph, an important parameter that has to be optimized is the T_{IN} of the first reactor. In order to do so, some simulation changing this parameter have been carried out, looking then at the plant performances.

For both reactor the N_T has been fixed to 708, number found in the precedent simulations, and the flow ratio value in the splitter has been fixed to 0.9930. Regarding the first reactor, the T_{cool} has been optimized in a way that the $T_{HotSpot}$ reaches the value previously set of 534 K.

EVALUATION OF THE CASES

T_{IN} 1° Reactor [K]	M_i [-]	RR [-]	MeOH Productivity [kmol/h]	Normalized CH_3OH Prod. Over Fresh Feed [-]	Overall CO_x Conversion χ %	1° Reactor CO_x Conversion χ %	2° Reactor CO_x Conversion χ %	T_{cool} [K]
348.15	0.796	1.818	265.12	0.3199	25.60	22.54	3.93	506.45
373.15	0.864	1.505	265.56	0.3205	29.90	25.28	6.18	504.75
403.15	0.931	1.256	265.98	0.3209	34.60	28.19	8.90	502.95
418.15	0.939	1.185	266.10	0.3211	35.54	28.57	9.75	502.55
433.15	0.902	1.197	266.07	0.3211	34.65	27.70	9.62	502.75
458.15	0.731	1.649	265.317	0.3202	26.23	22.22	5.15	506.05

Table 4.9 Process Performances for the Lurgi configuration with as fresh feed stream 2E.

Table 4.9 shows the performances achieved by the Lurgi configuration, varying the inlet temperature of the first reactor. Until 418.15 K, an increase in the T_{IN} results with an increase of the CO_x conversion and on the methanol productivity. Increasing further the temperature the performances get worse. Probably, as stated in the previous chapters, the excessive increase of T_{IN} leads to the not efficient usage of the last part of the reactor due to the thermodynamic limitations.

EVALUATION OF THE CASES

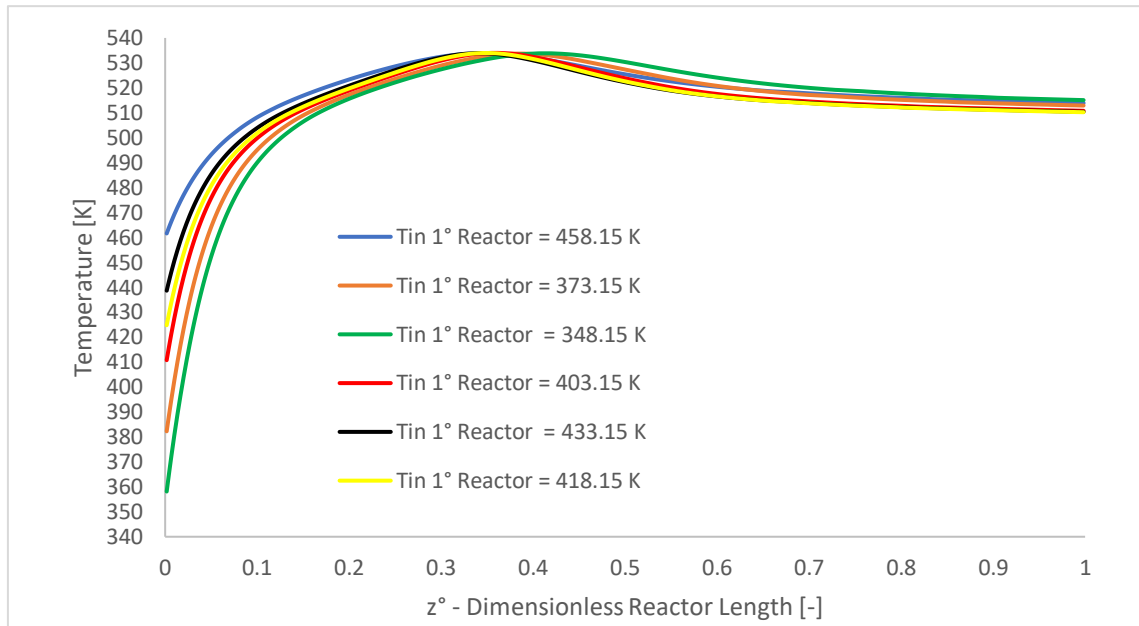


Figure 4.11 Temperature profile of the first reactor for a Lurgi configuration with a fresh feed stream 2E.

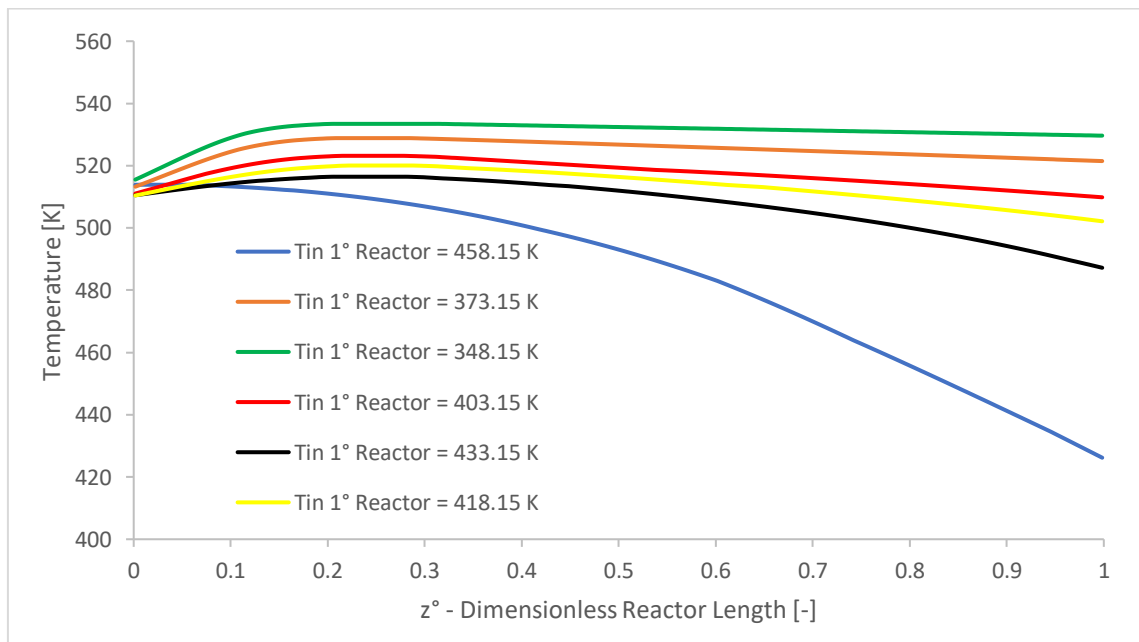


Figure 4.12 Temperature profile of the second reactor for a Lurgi configuration with a fresh feed stream 2E.

EVALUATION OF THE CASES

Figure 4.11 and Figure 4.12 show the temperature profile respectively of the first and second reactor. The former, as already seen, is the typical behaviour of a methanol reactor: initially the temperature increases thanks to the exchange with the coolant but then the reactions start and the temperature increases more, until reaching the maximum, where the heat absorbed by the coolant and the heat absorbed by the endothermicity of the reverse reactions force the temperature to approach the T_{cool} . As for what found in paragraph 4.2.3, the higher is the T_{IN} , the sooner the maximum temperature will be met. Despite the difference in T_{cool} and T_{IN} , the outlet temperatures of all the simulations realized are comparable.

The latter is the innovation brought from this loop. Depending on the T_{IN} of the first reactor, the behaviour in the second is different. In almost all the simulation (not the one with $T_{IN} 1^{\circ}$ reactor = 458.15 K) it is spotted a first part in which the temperature increase, due to the small extent of reaction not completed in the first reactor, but then, thanks to the coolant (that is the initial cold syngas that will be preheated before being fed to the first reactor), the temperature decreases, following the equilibrium behaviour, bringing an increasing of the CO_x conversion and of the methanol productivity.

For the configurations in which $T_{IN} 1^{\circ}$ Reactor is in the range of 340 – 410 K, the temperature increase is accentuated, meaning that the performances of the first reactor are not that good. Consequence of this is that the second reactor is not used to better follow the equilibrium conversion but actually to complete the job destined for the first reactor. For the other simulations, the temperature decrease is a good sign that the methanol percentage in the mixture is raising. Of course, as above mentioned, if the thermodynamic equilibrium is reached in the first reactor due to the too high initial temperature (when the last part of the reactor is not working), even though the temperature of the second reactor decreases, there will be no advantage in its availment.

4.3 Stream 2D simulation

In this paragraph, will be displayed all the simulations that consider as fresh feed stream 2D, a stream coming from the reforming of BIO_NG without the capture of CO₂. The main disadvantage of this stream is that the percentage of this component is so high that the modulus is very low, leading to excess of the CO_x and making the H₂ the limiting reactant. Starting from the data developed from [7], some parameters will be changed in order to optimize the performances of this synthesis loop.

4.3.1 Constant N_T

As in [7] and in the first simulation about stream 2E, the intent is to try to change just molar flow and composition of the fresh feed and see what happens to the reactor performances. The N_T will remain constant (4650 tubes) as well as all the other parameters such as T_{cool} and the flow ratio value used in the splitter.

The high CO_x content in the fresh feed means that the extent of reaction corresponds to the quantity of the limiting reactant that reacts. Therefore, in the first iteration, the quantity of CO_x reacted is very low, leading to their almost complete recycling. This, summed up at every loop iterations, leads to an increase in the RI molar flow rate. Starting from 1160 kmol/h as flow rate of the fresh feed, in the last iteration, the RI flow rate will be 80750 kmol/h that coincide with a flow rate per each tube that is excessively high and pressure drops of the order of 60 bar due to the exaggerated velocities. These number are unreal and the simulation will not be completed not even by the numerical simulator.

The reactor in this case is called, not active, in fact the temperature of the reactor increases in the first part of it thanks to the heat exchanged by the cooler, but then it remains constant to that level, revealing that almost no reaction is occurring.

EVALUATION OF THE CASES

4.3.2 Constant Reactor Inlet / N_T

What it can be done to avoid the aforementioned problems about the inactivity of the reactor leading also to high pressure drops, is to optimize, as already done with stream 2E, the N_T in a way that the ratio between the RI molar flow per each tube results constant. The goal value is, as found by [7], 3.877 kmol/h per each tube. In this case, seen that M_F is 0.232, the N_T will inevitably increase to contain the high flow rates expressed in the precedent paragraph. The value of this parameter found here is 8970 tubes.

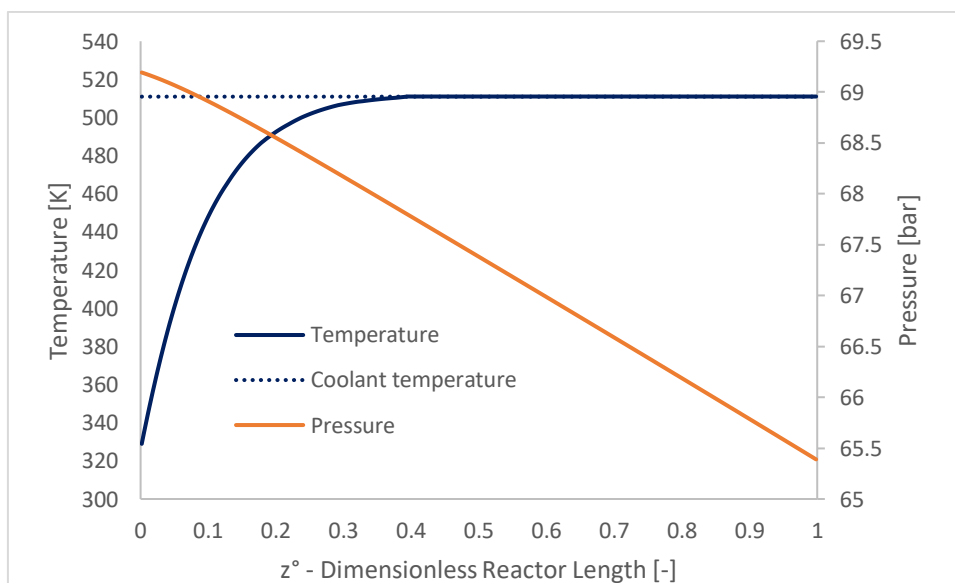


Figure 4.13 Temperature and Pressure profile at centerline vs reactor length for stream 2D with constant $RI/NT = 3.877$ kmol/h per each tube . Blue solid line: Temperature, blue pointed line: T_{cool} , red solid line: Pressure.

EVALUATION OF THE CASES

Figure 4.13 shows the temperature and pressure profile inside the reactor with stream 2D as fresh feed and with the optimization of the RI/N_T ratio. As clearly understandable, even though the increased number of tubes avoid the excessive pressure drops inside the reactor, the reactions don't start. The temperature raises to the coolant value and then remain constant. Proof of this is the CO_x conversion that is 0.71 %. The methanol productivity is 213 kmol/h but, if we compare this number with the RI flow rate (33950 kmol/h) it is evident that the reactor performances are undesirable. From a value of 0.232 in the fresh feed, when the latter is mixed with the recycle, the M_I reaches negative values. This means that the CO_2 present in the mixture is more than the H_2 , and this, as explained from chapter 2, must be avoided. All of these results are shown in Table 4.10 in which also the RR value is displayed. Of course, considering that no reaction is happening, almost all the vapor stream coming from the flash will be recycled, leading to high value of this parameter.

	Stream 2E with high inerts content in the RI
CO_x Conversion χ %	0.71
MeOH Productivity [kmol/h]	213.014
Normalized CH_3OH Prod. [-]	0.1836
RR [-]	28.27
M_I [-]	-0.5748
RI [kmol/h]	33950

Table 4.10 Performances for a reactor with stream 2D, with $RI/N_T = 3.877$ kmol/h per each tube.

There are no ways of optimizing this simulation without adding H_2 . Next step will be to try to optimize the process adding pure H_2 to the old RI and try to understand whether or not the process will be feasible.

EVALUATION OF THE CASES

4.3.3 Adding H₂

As in paragraph 4.2.3, the temperature profile of all the simulation implemented is shown in Figure 4.15. In this case, results are more difficult to be understood. The minimum H₂ added is 600 kmol/h, because a lower quantity would not help in the activation of the reactor and no improvements in the results presented in the previous simulation were noticed.

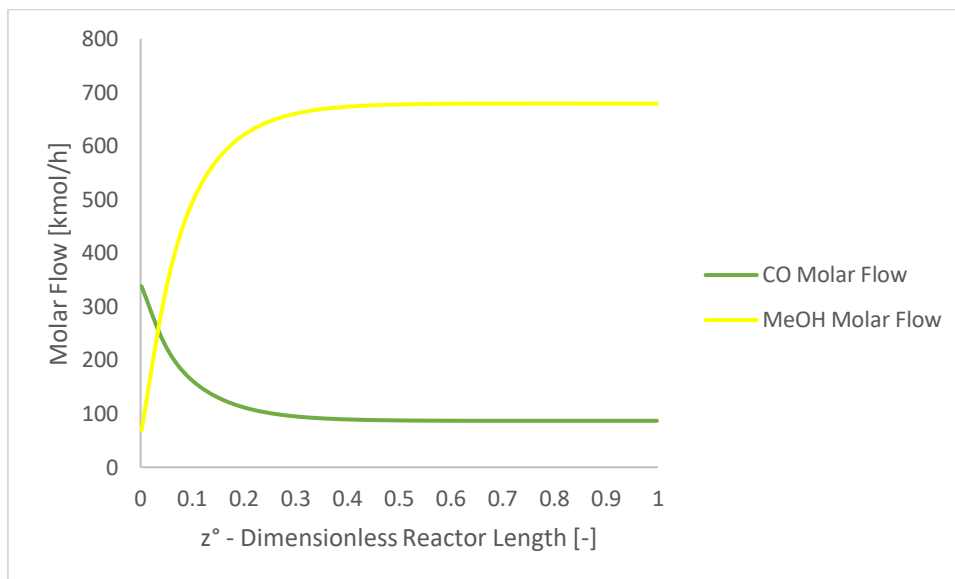


Figure 4.14 Methanol and CO molar flow inside the reactor at centerline, for the stream 2D adding 1300 kmol/h of H₂.

Despite what happen for the stream 2E, where no simulation reaches the equilibrium, in this case the situation is different. All of the cases presented here, display a plateau reached early in the reactor (before half of it) at the same temperature of the coolant one. This means either that no heat generation is present or that the heat generated from the reactions is equal to the heat absorbed by the coolant. This inference can be validate just looking at the methanol or CO molar flow inside the reactor. Figure 4.14 shows these behaviours inside the reactor just for the last simulation with 1300 kmol/h of H₂ added. After the first variability, both molar flows reach a plateau, meaning that no production/consumption of MeOH/CO is going on.

EVALUATION OF THE CASES

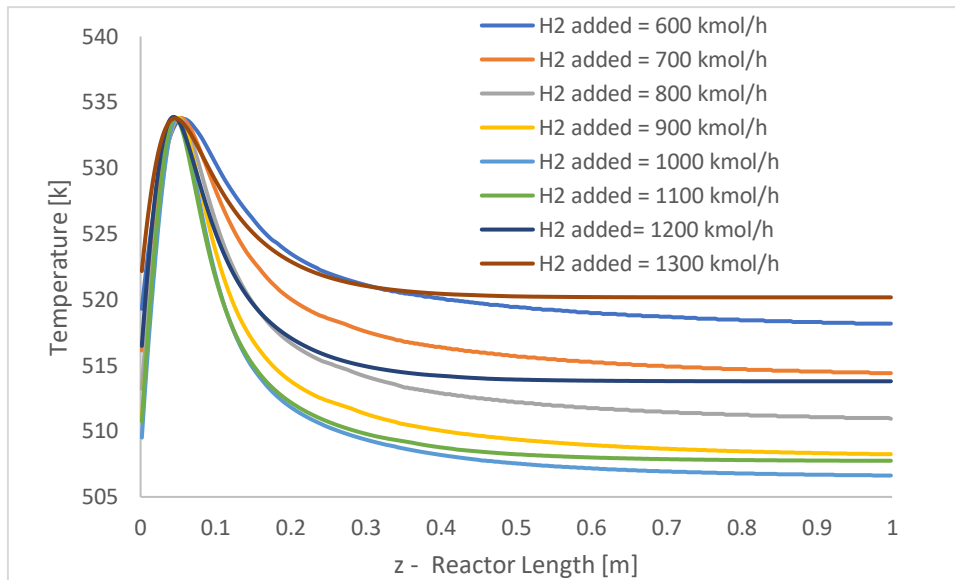


Figure 4.15 Temperature profile for a reactor with as fresh feed stream 2D and the addition of pure H₂ after the mixing with the recycle.

Looking at Table 4.11 to really understand which of these are the best in terms of performances, we can spot two different range:

- From 600 kmol/h to 1100 kmol/h of H₂ added, where the reactor ameliorates. M_I increases to values next to the optimal ones, CO_x conversion increase, due to the fact that H₂ is becoming less and less limiting, and methanol productivity (the normalized one too) increases as well. In this range, the addition of H₂ results to a benefit that has to be quantified by a profitability assessment.
- From 1100 kmol/h to 1300 kmol/h of H₂ added, where the addition of H₂ is actually a malus for the reactor performances. CO_xs are becoming the limiting reactants. In this case, the excess of H₂ will be recycled and will accumulate in the reactor leading to worsening of the methanol production and the other parameters.

Taking into account these considerations, the optimal simulation is the one in the range of the change between limiting agent. If the H₂ added is between 1000 kmol/h and 1100 kmol/h, the higher Normalized Methanol Productivity is noticed.

EVALUATION OF THE CASES

	H ₂ added [kmol/h]	RR [-]	M _i [-]	CO _x Conversion χ %	MeOH Productivity [kmol/h]	Normalized CH ₃ OH Prod. Over Fresh Feed [-]	Normalized CH ₃ OH Prod. Over Fresh Feed + H ₂ [-]	RI molar flow (adding H ₂) [kmol/h]	T _{IN} = T _{cool} [K]
1	600	4.72	-7.9 *10 ⁻³	11.87	451.01	0.389	0.2562	6633 (7233)	517.35
2	700	3.98	0.35	16.98	484.55	0.4177	0.2605	6472 (5772)	513.75
3	800	3.59	0.84	23.43	517.55	0.4461	0.2640	5321 (6121)	510.45
4	900	3.50	1.57	31.58	549.67	0.4739	0.2668	5222 (6122)	507.85
5	1000	3.81	2.79	41.51	580.52	0.5	0.2687	5582 (6582)	506.45
6	1100	5.06	5.34	54.61	607.56	0.5238	0.2688	7035 (8135)	507.65
7	1200	8.91	11.46	66.15	623.59	0.5376	0.2642	11500 (12700)	513.75
8	1300	15.4	19.63	71.54	628.68	0.542	0.2556	19020 (20320)	520.15

Table 4.11 Performances for a reactor with stream 2D when different quantities of pure H₂ are added.

EVALUATION OF THE CASES

5

Conclusion

As I mentioned in the beginning of this work, the usage of renewable energy sources is becoming fundamental in the new energy scenario. Fossil fuels are starting to diminish and it is not safe to completely rely on them. After a small literature research on how biomasses energy can be exploited and use through their gasification, simulations about methanol synthesis starting from renewable syngas were implemented. The validation of the model, comparing it with the work proposed by [7], is the first result we obtained. Starting from a feed rich in H_2 and CO , with a multitubular reactor, in which boiling water and reactants flow respectively in the shell and in the tubes, the transformation of the syngas to methanol was completed. Due to the low per pass conversion, a purge and a recycle was inserted in the loop. The stoichiometric coefficient of this case was in the range of the optimal one (2.109 in the fresh feed). This lead to high methanol yield. The value of the normalized yield is equal to 0.3219 and will be the set one to understand if the methanol produced from the simulations carried out subsequently is in an interesting quantity. Next there was the model improvement, in which no more ideal flash were used, but a real condenser based on real case example data. 0.3083 is the value of the normalized methanol productivity, lower than before as expected if the efficiency of the separation section is decreased. Two different stream coming from the gasification of biomass were investigated: stream 2E, coming from the reforming + capture of the CO_2 of bio-natural gas, that has a stoichiometric coefficient equal to 1.790; stream 2D, coming from the reforming of bio-natural gas, that is rich in CO_2 and has a stoichiometric coefficient equal to 0.232.

Regarding stream 2E, not all the simulation presented in chapter 4 are of interest in the methanol scenarios. The simulation in which we keep constant all the parameter, as in the validate model, and change flow and composition of the fresh feed, lead to a too hot reactor that is not practicable.

Second case is when we consider constant the ratio between the reactor inlet flow rate and the number of the tubes. Setting this number to 3.877 kmol/h per each tube we search for the solution that optimizes the methanol productivity without working in a dangerous environment. Decreasing the coolant temperature

CONCLUSIONS

to 507.15 K and working with the inlet temperature of the reactor equal to 323 K, we reach good performances. 0.3168 is the value of the normalized methanol productivity, the hotspot temperature is not excessively high and is below the limit (set to 540 K to avoid methanation and loss in catalyst activity), and the value of recycle ratio are reasonable and will not lead to exaggerated cost for the recycling.

Next case is the one in which we try to use the first part of the reactor not to heat up the reactants but to actually help in the transformation of them. Increasing the inlet temperature of the reactor to 508.55 K and setting equal to this value also the coolant temperature we obtain 0.3195 as normalized methanol productivity. Considering that also in this case the hotspot temperature is still below the limit even though is 4 degrees higher than the previous one and the recycle ratio are in order of 2 we can set this simulation as acceptable.

From now on, all the simulation will be carried out fixing the hotspot temperature to 534 K in order to be able to compare them.

Simulations in which pure hydrogen is added to the mix between the initial fresh feed and the recycle of the reactor were also implemented. Different amount of hydrogen added were simulated. The best configuration is the one that involve 20 kmol/h of hydrogen that lead to a normalized methanol productivity of 0.3209 (calculated as the quantity of methanol produced divided by the sum of all the flows that enter the "black box") and a recycle ratio equal to 1.5 that is lower than the previous simulations.

Last simulation about stream 2E is the one that involve two reactors in series. All the parameters in both of them are fixed as in the other simulations and their coupling is discussed in chapter 4. The best configuration is the one that consider as inlet temperature of the first reactor 433.15 K that leads to 0.3211 as normalized methanol productivity and 1.197 as recycle ratio.

Regarding stream 2D, the simulations carried out without the usage of pure hydrogen led to a not active reactor, indicating very bad performances and flat temperature profiles. Adding H₂ helped in the activation of the reactor (bringing the mixture with a stoichiometric coefficient in the range of the optimal one). In particular the simulation in which 1100 kmol/h of pure H₂ were added has 0.2688 as normalized methanol productivity and 5.06 as recycle ratio value. These numbers are lower if we compare them to the aforementioned one about the simulations carried out on the stream 2E but is still something if we think of the amount of CO₂ present in the fresh feed.

With just these parameters it is not possible to tell which one of these configurations is the best. Quantity of methanol produced, CO_x conversion, recycle ratio etc. have to be coupled with an economical assessment of the plant, in order to understand if CAPEX and OPEX of the configurations can be repaid with the sale of products and by products. Moreover, Net Present Value and Payback Time, are two important parameters useful to understand if the investment made is profitable and their calculation could help in the decision.

CONCLUSIONS

Future developments

The simulations carried out in this work spotted a good behaviour of the plant scheme to the feeds produced from the gasification of biomasses. However, some of the assumption made in the beginning of chapter 3 can be overtaken leading to more accurate results.

First of all, the consideration of the catalyst efficiency as constant is a strong assumption. The inclusion of a separated model to calculate it at each point in the reactor length could be useful to really optimize the reaction rate values.

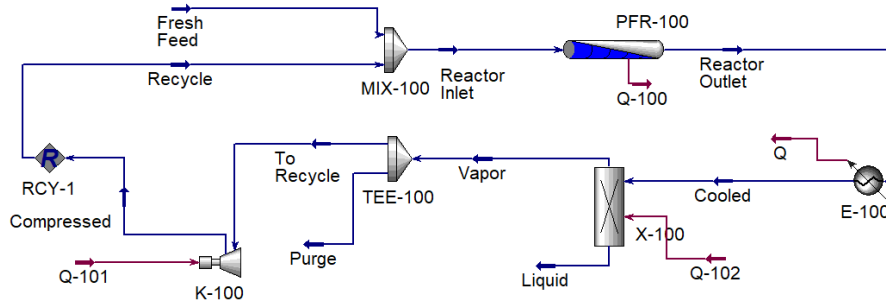
The simulations were made neglecting the solid catalyst phase. Its modelling could help in better understand the behaviour of the heat exchanged and could help in the identification of the optimal coolant and inlet temperature of the reactor.

Least, the radial dispersion of the heat could be simulated in order to avoid overperformances of the heat exchanged that in turn lead to overperformances of the reactor regarding the methanol productivity.

CONCLUSIONS

Appendix A

Validate Model Workbook and flowsheet



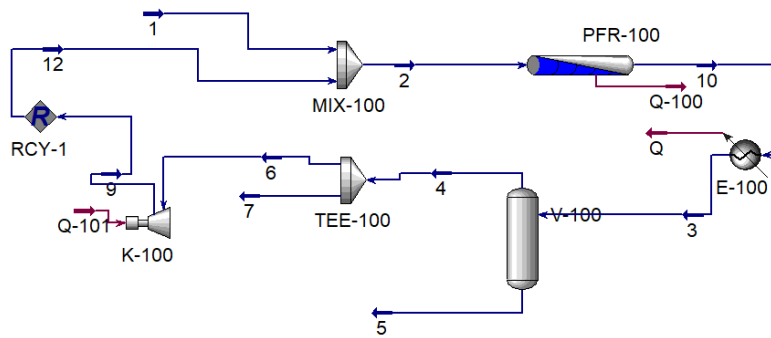
	Unit	Fresh Feed	Vapor	To Recycle	Purge	Compressor	Reactor Out	Reactor Inlet	Recycle	Cooled	Liquid
Vapour Fraction		1	1	1	1	1	1	1	1	0.905422	0
Temperature	C	87.1265	37	37	37	38.11634	238.5896	49.85	38.11635	37	37
Pressure	kPa	6920	6854.342	6854.342	6854.342	6920	6854.342	6920	6920	6854.342	6854.342
Molar Flow	kgmole/h	4360.426	13855.33	13669.66	185.6614	13669.66	15348.37	18030	13669.57	15348.37	1493.042
Mass Flow	kg/h	46557.37	63673.44	62820.22	853.2241	62820.22	109381	109377.6	62820.21	109381	45707.54
Liquid Volume Flow	m ³ /h	137.5127	445.3663	439.3983	5.967908	439.3983	502.1104	576.9082	439.3955	502.1104	56.74419
Heat Flow	kJ/h	-1.9E+08	-2.2E+08	-2.1E+08	-2891850	-2.1E+08	-4.2E+08	-4E+08	-2.1E+08	-5.8E+08	-3.7E+08
Comp Mole Frac (CO)		0.273203	0.012946	0.012946	0.012946	0.012946	0.011686	0.075888	0.012946	0.011686	0
Comp Mole Frac (CO ₂)		0.0355	0.015095	0.015095	0.015095	0.015095	0.013627	0.020031	0.015096	0.013627	0
Comp Mole Frac (Hydrogen)		0.686408	0.857239	0.857239	0.857239	0.857239	0.77385	0.815925	0.857239	0.77385	0
Comp Mole Frac (H ₂ O)		0	0	0	0	0	0.009905	0	0	0.009905	0.101819
Comp Mole Frac (Methanol)		0	0	0	0	0	0.087372	0	0	0.087372	0.898181
Comp Mole Frac (Methane)		0.004888	0.11472	0.11472	0.11472	0.11472	0.10356	0.088157	0.114719	0.10356	0

	Unit	Q-100	Q-101	Q	Q-102
Heat Flow	kJ/h	23702854	466872.8	1.58E+08	-2365354

APPENDICES

Appendix B

Improved Model Workbook and flowsheet



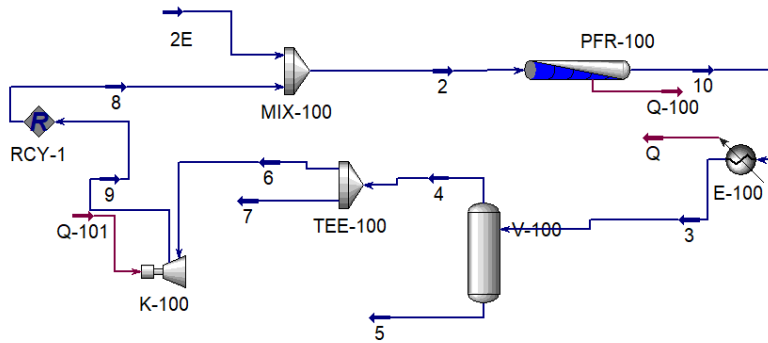
	Unit	1	3	4	5	6	7	9	10	2	12
Vapour Fraction		1	0.977129	1	0	1	1	1	1	1	1
Temperature	C	227.8	37	37	37	37	37	37.80568	237.8718	49.85	37.80568
Pressure	kPa	6920	6872.935	6872.935	6872.935	6872.935	6872.935	6920	6872.935	6920	6920
Molar Flow	kgmole/h	1144.843	17323.69	16927.48	396.2056	16885.16	42.31871	16885.16	17323.69	18030	16885.16
Mass Flow	kg/h	12223.77	72153.62	60080.65	12072.98	59930.44	150.2016	59930.44	72153.62	72153.97	
Liquid Volume Flow	m ³ /h	36.10435	544.1693	529.1029	15.06643	527.7801	1.322757	527.7801	544.1693	563.8839	527.7795
Heat Flow	kJ/h	-4.4E+07	-2.3E+08	-1.4E+08	-9.7E+07	-1.4E+08	-339779	-1.4E+08	-1.1E+08	-1.8E+08	-1.4E+08
Comp Mole Frac (CO)		0.273203	0.002297	0.002351	2.31E-05	0.002351	0.002351	0.002351	0.002297	0.019549	0.002351
Comp Mole Frac (CO ₂)		0.0355	0.000673	0.000682	0.000312	0.000682	0.000682	0.000682	0.000673	0.002893	0.000682
Comp Mole Frac (Hydrogen)		0.686408	0.878249	0.898746	0.002534	0.898746	0.898746	0.898746	0.878249	0.885264	0.898747
Comp Mole Frac (H ₂ O)		0	0.002514	0.000182	0.102175	0.000182	0.000182	0.000182	0.002514	0.00017	0.000182
Comp Mole Frac (Methanol)		0	0.024374	0.004092	0.890908	0.004092	0.004092	0.004092	0.024374	0.003832	0.004092
Comp Mole Frac (Methane)		0.004888	0.091892	0.093948	0.004048	0.093948	0.093948	0.093948	0.091892	0.088292	0.093947

	Unit	Q-100	Q-101	Q
Heat Flow	kJ/h	-6.9E+07	412895.4	1.23E+08

APPENDICES

Appendix C

Stream 2E with $T_{IN} = 323\text{ K}$ and $T_{cool} = 507.15\text{ K}$ Workbook and flowsheet



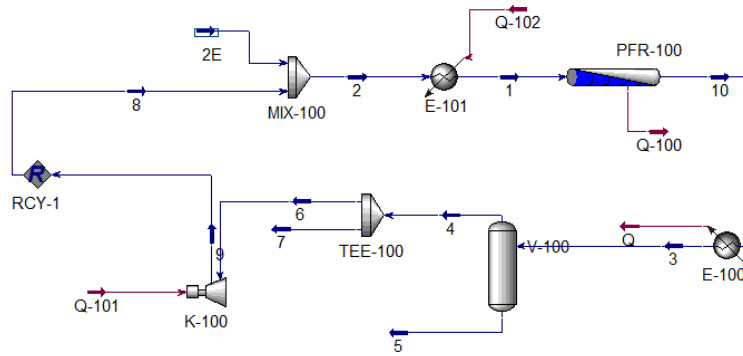
	Unit	3	4	5	6	7	9	10	2	8	2E
Vapour Fraction		0.874973	1	0	1	1	1	1	1	1	1
Temperature	C	37	37	37	37	37	37.09459	238.5132	49.85	37.09459	90.14523
Pressure	kPa	6914.116	6914.116	6914.116	6914.116	6914.116	6920	6914.116	6920	6920	6920
Molar Flow	kgmole/h	2340.58	2047.945	292.6356	2046.921	1.023972	2046.921	2340.58	2875.504	2046.904	828.6
Mass Flow	kg/h	61180.89	51632.88	9548.009	51607.07	25.81644	51607.07	61180.89	61180.46	51606.64	9573.821
Liquid Volume Flow	m3/h	88.107	76.12177	11.98523	76.08371	0.038061	76.08371	88.107	102.1914	76.0831	26.10835
Heat Flow	kJ/h	-2.8E+08	-2E+08	-7.3E+07	-2E+08	-101380	-2E+08	-2.5E+08	-2.4E+08	-2E+08	-3.6E+07
Comp Mole Frac (CO)		0.315991	0.360482	0.004637	0.360482	0.360482	0.360482	0.315991	0.34968	0.360481	0.323
Comp Mole Frac (CO2)		0.129692	0.138947	0.064917	0.138947	0.138947	0.138947	0.129692	0.106113	0.138948	0.025
Comp Mole Frac (Hydrogen)		0.154318	0.17626	0.000768	0.17626	0.17626	0.17626	0.154318	0.312196	0.17626	0.648
Comp Mole Frac (H2O)		0.000694	1.85E-05	0.005424	1.85E-05	1.85E-05	1.85E-05	0.000694	1.32E-05	1.85E-05	0
Comp Mole Frac (Methanol)		0.12041	0.007005	0.914053	0.007005	0.007005	0.007005	0.12041	0.004986	0.007005	0
Comp Mole Frac (Methane)		0.034598	0.039157	0.002693	0.039157	0.039157	0.039157	0.034598	0.028162	0.039157	0.001
Comp Mole Frac (Nitrogen)		0.244296	0.278131	0.007509	0.278131	0.278131	0.278131	0.244296	0.19885	0.278132	0.003
Comp Mole Frac (Oxygen)		0	0	0	0	0	0	0	0	0	0
Comp Mole Frac (Ethane)		0	0	0	0	0	0	0	0	0	0
Comp Mole Frac (Propane)		0	0	0	0	0	0	0	0	0	0
Comp Mole Frac (n-Butane)		0	0	0	0	0	0	0	0	0	0

	Unit	Q-100	Q-101	Q
Heat Flow	kJ/h	9326283	5985.364	27351630

APPENDICES

Appendix D

Stream 2E with $T_{IN} = T_{cool} = 508.55$ K Workbook and flowsheet



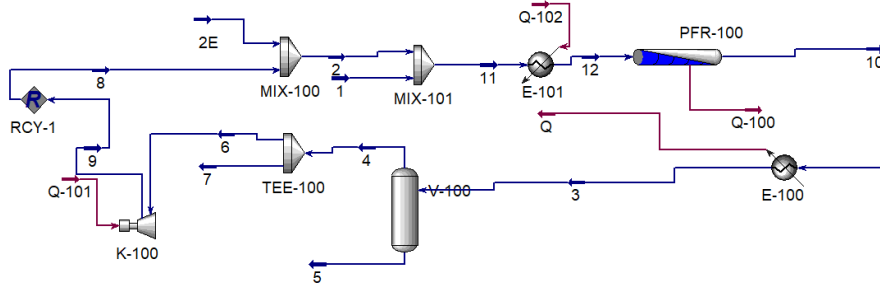
	Unit	3	4	5	6	7	9	10	2	8	2E	1
Vapour Fraction		0.863238	1	0	1	1	1	1	1	1	1	1
Temperature	C	37	37	37	37	37	39.98317	242.5961	42.25831	39.98311	49.85	235.4
Pressure	kPa	6740.291	6740.291	6740.291	6740.291	6740.291	6920	6740.291	6920	6920	6920	6920
Molar Flow	kgmole/h	2097.408	1810.563	286.8451	1797.889	12.67394	1797.889	2097.408	2626.47	1797.87	828.6	2626.47
Mass Flow	kg/h	48114.31	38812.79	9301.519	38541.1	271.6895	38541.1	48114.31	48114.54	38540.72	9573.821	48114.54
Liquid Volume Flow	m3/h	76.38516	64.71778	11.66738	64.26476	0.453024	64.26476	76.38516	90.37244	64.26409	26.10835	90.37244
Heat Flow	kJ/h	-2.4E+08	-1.7E+08	-7.1E+07	-1.7E+08	-1205320	-1.7E+08	-2.2E+08	-2.1E+08	-1.7E+08	-3.7E+07	-1.9E+08
Comp Mole Frac (CO)		0.354722	0.410136	0.004945	0.410136	0.410136	0.410136	0.354722	0.382646	0.410136	0.323	0.382646
Comp Mole Frac (CO2)		0.109513	0.118194	0.054719	0.118194	0.118194	0.118194	0.109513	0.088793	0.118194	0.025	0.088793
Comp Mole Frac (Hydrogen)		0.271581	0.314409	0.00125	0.314409	0.314409	0.314409	0.271581	0.41965	0.314409	0.648	0.41965
Comp Mole Frac (H2O)		0.00171	3.77E-05	0.012269	3.77E-05	3.77E-05	3.77E-05	0.00171	2.58E-05	3.77E-05	0	2.58E-05
Comp Mole Frac (Methanol)		0.131567	0.00635	0.921932	0.00635	0.00635	0.00635	0.131567	0.004347	0.00635	0	0.004347
Comp Mole Frac (Methane)		0.023131	0.026524	0.001716	0.026524	0.026524	0.026524	0.023131	0.018471	0.026524	0.001	0.018471
Comp Mole Frac (Nitrogen)		0.107776	0.124349	0.003169	0.124349	0.124349	0.124349	0.107776	0.086066	0.12435	0.003	0.086066
Comp Mole Frac (Oxygen)		0	0	0	0	0	0	0	0	0	0	0
Comp Mole Frac (Ethane)		0	0	0	0	0	0	0	0	0	0	0
Comp Mole Frac (Propane)		0	0	0	0	0	0	0	0	0	0	0
Comp Mole Frac (n-Butane)		0	0	0	0	0	0	0	0	0	0	0

	Unit	Q-100	Q-101	Q	Q-102
Heat Flow	kJ/h	25852301	165727.3	25616936	16050530

APPENDICES

Appendix E

Stream 2E with 20 kmol/h of pure Hydrogen added Workbook and flowsheet



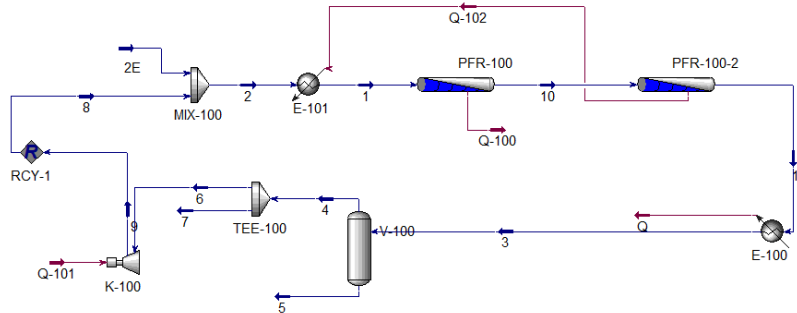
	Unit	3	4	5	6	7	9	10	2	8	2E	1	11	12
Vapour Fraction		0.80941	1	0	1	1	1	1	1	1	1	1	1	1
Temperature	C	37	37	37	37	37	38.31331	234.9464	42.55214	38.3133	49.85	40	42.49991	227.9
Pressure	kPa	6841.407	6841.407	6841.407	6841.407	6841.407	6920	6841.407	6920	6920	6920	6920	6920	6920
Molar Flow	kgmole/h	1548.653	1253.494	295.1582	1244.72	8.774461	1244.72	1548.653	2073.315	1244.715	828.6	20	2093.315	2093.315
Mass Flow	kg/h	28991.27	19514.04	9477.231	19377.44	136.5983	19377.44	28991.27	28951.16	19377.34	9573.821	40.32	28991.48	28991.48
Liquid Volume Flow	m ³ /h	54.54525	42.65964	11.88561	42.36102	0.298617	42.36102	54.54525	68.46919	42.36084	26.10835	0.577162	69.04635	69.04635
Heat Flow	kJ/h	-1.5E+08	-7.6E+07	-7.3E+07	-7.6E+07	-535044	-7.6E+07	-1.3E+08	-1.1E+08	-7.6E+07	-3.7E+07	10341.94	-1.1E+08	-1E+08
Comp Mole Frac (CO)		0.159851	0.196944	0.002321	0.196944	0.196944	0.196944	0.159851	0.247322	0.196943	0.323	0	0.244959	0.244959
Comp Mole Frac (CO ₂)		0.082266	0.091423	0.043378	0.091423	0.091423	0.091423	0.082266	0.064877	0.091423	0.025	0	0.064257	0.064257
Comp Mole Frac (Hydrogen)		0.422707	0.521779	0.001964	0.521779	0.521779	0.521779	0.422707	0.572224	0.521778	0.648	1	0.576311	0.576311
Comp Mole Frac (H ₂ O)		0.004641	6.29E-05	0.024083	6.29E-05	6.29E-05	6.29E-05	0.004641	3.78E-05	6.29E-05	0	0	3.74E-05	3.74E-05
Comp Mole Frac (Methanol)		0.180333	0.005576	0.922503	0.005576	0.005576	0.005576	0.180333	0.003348	0.005576	0	0	0.003316	0.003316
Comp Mole Frac (Methane)		0.025009	0.03045	0.001902	0.03045	0.03045	0.03045	0.025009	0.01868	0.03045	0.001	0	0.018502	0.018502
Comp Mole Frac (Nitrogen)		0.125192	0.153765	0.003848	0.153765	0.153765	0.153765	0.125192	0.093512	0.153765	0.003	0	0.092618	0.092618
Comp Mole Frac (Oxygen)		0	0	0	0	0	0	0	0	0	0	0	0	0
Comp Mole Frac (Ethane)		0	0	0	0	0	0	0	0	0	0	0	0	0
Comp Mole Frac (Propane)		0	0	0	0	0	0	0	0	0	0	0	0	0
Comp Mole Frac (n-Butane)		0	0	0	0	0	0	0	0	0	0	0	0	0

	Unit	Q-100	Q-101	Q	Q-102
Heat Flow	kJ/h	26579781	50370.15	21689243	11961844

APPENDICES

Appendix F

Stream 2E Lurgi configuration with T_{IN} 1° Reactor = 433.15 K Workbook and flowsheet



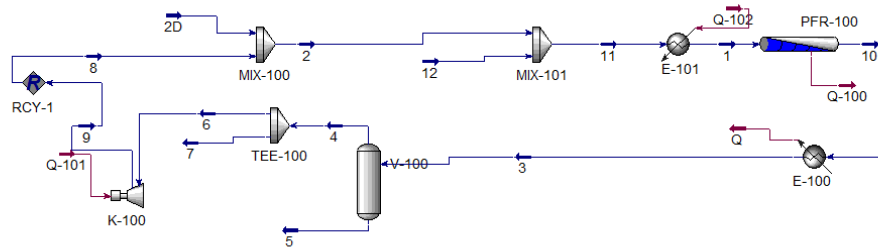
	Unit	3	4	5	6	7	9	10	2	8	2E	1	11
Vapour Fraction		0.775344	1	0	1	1	1	1	1	1	1	1	1
Temperature	C	37	37	37	37	37	39.36405	237.2202	43.04154	39.36403	49.85	160	214.0657
Pressure	kPa	6776.345	6776.345	6776.345	6776.345	6776.345	6920	6841.654	6920	6920	6920	6920	6776.345
Molar Flow	kgmole/h	1288.172	998.7757	289.3959	991.7842	6.99143	991.7842	1394.551	1820.38	991.7805	828.6	1820.38	1288.172
Mass Flow	kg/h	31138.52	21716.97	9421.551	21564.95	152.0188	21564.95	31138.57	31138.7	21564.87	9573.821	31138.7	31138.52
Liquid Volume Flow	m ³ /h	47.86334	36.03893	11.82441	35.78666	0.252273	35.78666	50.6313	61.89487	35.78652	26.10835	61.89487	47.86334
Heat Flow	kJ/h	-1.7E+08	-9.4E+07	-7.2E+07	-9.3E+07	-656630	-9.3E+07	-1.4E+08	-1.3E+08	-9.3E+07	-3.7E+07	-1.2E+08	-1.5E+08
Comp Mole Frac (CO)		0.27476	0.353106	0.004367	0.353106	0.353106	0.353106	0.29253	0.339402	0.353106	0.323	0.339402	0.27476
Comp Mole Frac (CO ₂)		0.114587	0.130165	0.060824	0.130165	0.130165	0.130165	0.105257	0.082296	0.130164	0.025	0.082296	0.114587
Comp Mole Frac (Hydrogen)		0.23888	0.307729	0.001264	0.307729	0.307729	0.307729	0.29635	0.462613	0.307728	0.648	0.462613	0.23888
Comp Mole Frac (H ₂ O)		0.001728	2.38E-05	0.00761	2.38E-05	2.38E-05	2.38E-05	0.002185	1.30E-05	2.38E-05	0	1.30E-05	0.001728
Comp Mole Frac (Methanol)		0.211552	0.006459	0.919375	0.006459	0.006459	0.006459	0.157273	0.003519	0.006459	0	0.003519	0.211552
Comp Mole Frac (Methane)		0.024868	0.031464	0.002103	0.031464	0.031464	0.031464	0.022971	0.017598	0.031465	0.001	0.017598	0.024868
Comp Mole Frac (Nitrogen)		0.133626	0.171052	0.004458	0.171052	0.171052	0.171052	0.123433	0.094559	0.171053	0.003	0.094559	0.133626
Comp Mole Frac (Oxygen)		0	0	0	0	0	0	0	0	0	0	0	0
Comp Mole Frac (Ethane)		0	0	0	0	0	0	0	0	0	0	0	0
Comp Mole Frac (Propane)		0	0	0	0	0	0	0	0	0	0	0	0
Comp Mole Frac (n-Butane)		0	0	0	0	0	0	0	0	0	0	0	0

	Unit	Q-100	Q-101	Q	Q-102
Heat Flow	kJ/h	16868709	72633.85	18691289	6683697

APPENDICES

Appendix G

Stream 2D with 1100 kmol/h of pure Hydrogen added Workbook and flowsheet



	Unit	3	4	5	6	7	9	10	2	8	2D	1	11	12
Vapour Fraction		0.858488	1	0	1	1	1	1	1	1	1	1	1	1
Temperature	C	37	37	37	37	37	37.08248	234.5995	49.85	37.08248	110.2991	234.5	48.41346	40
Pressure	kPa	6915.142	6915.142	6915.142	6915.142	6915.142	6920	6915.142	6920	6920	6920	6920	6920	6920
Molar Flow	kgmole/h	6919.937	5940.686	979.2516	5875.338	65.34754	5875.338	6919.937	7035.306	5875.306	1160	8135.306	8135.306	1100
Mass Flow	kg/h	64520.85	37814.43	26706.42	37398.47	415.9587	37398.47	64520.85	62302.21	37398.35	24903.86	64519.81	64519.81	2217.6
Liquid Volume Flow	m3/h	217.5833	185.6282	31.95516	183.5863	2.04191	183.5863	217.5833	227.8761	183.5853	44.29081	259.62	259.62	31.7439
Heat Flow	kJ/h	-4.4E+08	-1.8E+08	-2.5E+08	-1.8E+08	-2000663	-1.8E+08	-3.5E+08	-3.5E+08	-1.8E+08	-1.7E+08	-3.1E+08	-3.5E+08	568806.8
Comp Mole Frac (CO)		0.009078	0.010564	6.26E-05	0.010564	0.010564	0.010564	0.009078	0.045756	0.010564	0.224	0.039569	0.039569	0
Comp Mole Frac (CO2)		0.063934	0.070861	0.021916	0.070861	0.070861	0.070861	0.063934	0.112434	0.070861	0.323	0.097232	0.097232	0
Comp Mole Frac (Hydrogen)		0.746506	0.869366	0.001165	0.869366	0.869366	0.869366	0.746506	0.80022	0.869366	0.45	0.827233	0.827233	1
Comp Mole Frac (H2O)		0.050888	0.000602	0.355953	0.000602	0.000602	0.000602	0.050888	0.000502	0.000602	0	0.000434	0.000434	0
Comp Mole Frac (Methanol)		0.090408	0.003047	0.620392	0.003047	0.003047	0.003047	0.090408	0.002544	0.003047	0	0.0022	0.0022	0
Comp Mole Frac (Methane)		0.013399	0.015583	0.000144	0.015583	0.015583	0.015583	0.013399	0.013179	0.015583	0.001	0.011397	0.011397	0
Comp Mole Frac (Nitrogen)		0.025787	0.029977	0.000367	0.029977	0.029977	0.029977	0.025787	0.025364	0.029977	0.002	0.021934	0.021934	0
Comp Mole Frac (Oxygen)		0	0	0	0	0	0	0	0	0	0	0	0	0
Comp Mole Frac (Ethane)		0	0	0	0	0	0	0	0	0	0	0	0	0
Comp Mole Frac (Propane)		0	0	0	0	0	0	0	0	0	0	0	0	0
Comp Mole Frac (n-Butane)		0	0	0	0	0	0	0	0	0	0	0	0	0

	Unit	Q-100	Q-101	Q	Q-102
Heat Flow	kJ/h	46913265	14751.35	82837880	46327130

APPENDICES

6

Bibliography

- [1] Renewable Energy, by Edited by Godfrey Boyle, pp. 456. Oxford University Press, May 2004. ISBN-10: 0199261784. ISBN-13: 9780199261789
- [2] Maui Electric, <https://www.mauielectric.com/clean-energy-hawaii/clean-energy-facts>
- [3] Methanol Institute, The Methanol Industry, (2017), <http://www.methanol.org/the-methanol-industry/>.
- [4] The essential chemical industry – online, <http://www.essentialchemicalindustry.org/chemicals/methanol.html>
- [5] Cetiner Engineering Corporation, <http://cetiner.tripod.com/Methanolds.htm>
- [6] Modeling of a Methanol Synthesis Reactor for Storage of Renewable Energy and Conversion of CO₂ – Comparison of Two Kinetic Models Johannes J. Meyer, Pepe Tan, Andreas Apfelbacher, Robert Daschner, Andreas Hornung, <https://doi.org/10.1002/ceat.201500084>
- [7] Enabling small-scale methanol synthesis reactors through the adoption of highly conductive structured catalysts: AndreaMontebelli, Carlo GiorgioVisconti, GianpieroGroppi, EnricoTronconi, CristinaFerreira, StefanieKohler. <https://doi.org/10.1016/J.CATTOD.2013.02.020>
- [8] AspenTechnology.Inc, 2009. AspenTechnology.Inc. Aspen Energy Analyzer Reference Guide, 2009.
- [9] AspenTechnology.Inc, 2000. AspenTechnology.Inc. Aspen Plus User Guide, 2000.
- [10] B. Kummamuru, WBA Global Bioenergy Statistics 2016, Report (World Bioenergy Association, 2016).
- [11] Biomass feedstock supply chain network design with biomass conversion incentives N. Muhammad, AslaamMohamed Abdul Ghani, ChrysafisVogiatzis, JosephSzmerekovsky <https://doi.org/10.1016/j.enpol.2018.01.042>
- [12] Abuadala AG. Investigation of sustainable hydrogen production from steam biomass gasification; 2010.
- [13] S.G. Gopaul, A. Dutta, R. ClemmerChemical looping gasification for hydrogen production: a comparison of two unique processes simulated using ASPEN Plus Int J Hydrog Energy, 39 (2014), pp. 5804-5817

BIBLIOGRAPHY

- [14] A. Molino, S. Chianese, and D. Musmarra, Biomass gasification technology: The state of the art overview, *Journal of Energy Chemistry* 25, 10 (2016).
- [15] S. Basu, A. L. Khan, A. Cano-Odena, C. Liu, and I. F. J. Vankelecom, Membrane-based technologies for biogas separations, *Chemical Society Reviews* 39, 750 (2010).
- [16] Ullmann's Encyclopedia of Industrial Chemistry, Publisher: VCH
- [17] Moulijn, J., Makkee, M., van Diepen, A., *Chemical Process Technology*, Publisher: J. Wiley, 2001
- [18] M. Santiago, K. Barbera, C. Ferreira, D. Curulla-Ferré, P. Kolb, J. Pérez-Ramírez, *Catalysis Communications* 21 (2012) 63–67.
- [19] E. Fiedler, G. Grossmann, D.B. Kersebohm, G. Weiss, C. Witte, Methanol, in: Ullmann's Encyclopedia of Industrial Chemistry, 6th ed., Wiley-VCH GmbH, Weinheim, 2003, p. 611.
- [20] Maity, S.K., 2015. Opportunities, recent trends and challenges of integrated biorefinery: Part II. *Renew. Sustain. Energy Rev.* 43, 1446–1466. <http://dx.doi.org/10.1016/j.rser.2014.08.075>.
- [21] McKendry, P., 2002. Energy production from biomass (part 2): Conversion technologies. *Bioresour. Technol.* 83, 47–54. [http://dx.doi.org/10.1016/S0960-8524\(01\)00119-5](http://dx.doi.org/10.1016/S0960-8524(01)00119-5).
- [22] Sikarwar, V.S., Zhao, M., Clough, P., Yao, J., Zhong, X., Memon, M.Z., Shah, N., Anthony, E., Fennell, P., 2016. An overview of advances in biomass gasification. *Energy Environ. Sci.* 9, 2939–2977. <http://dx.doi.org/10.1039/C6EE00935B>.
- [23] Weiland, F., Hedman, H., Marklund, M., Wiinikka, H., Öhrman, O., Gebart, R., 2013. Pressurized oxygen blown entrained-flow gasification of wood powder. *Energy Fuels* 27, 932–941. <http://dx.doi.org/10.1021/ef301803s>.
- [24] Weiland, F., Wiinikka, H., Hedman, H., Wennebro, J., Pettersson, E., Gebart, R., 2015. Influence of process parameters on the performance of an oxygen blown entrained flow biomass gasifier. *Fuel* 153, 510–519. <http://dx.doi.org/10.1016/j.fuel.2015.03.041>.
- [25] Ma, C., Backman, R., Öhman, M., 2015. Thermochemical equilibrium study of slag formation during pressurized entrained-flow gasification of woody biomass. *Energy Fuels* 29, 4399–4406. <http://dx.doi.org/10.1021/acs.energyfuels.5b00889>.
- [26] Ma, C., Carlborg, M., Hedman, H., Wennebro, J., Weiland, F., Wiinikka, H., Backman, R., Öhman, M., 2016. Ash formation in pilot-scale pressurized entrained-flow gasification of bark and a bark/peat mixture. *Energy Fuels* 3. <http://dx.doi.org/10.1021/acs.energyfuels.6b02222>.
- [27] Carlsson, P., Ma, C., Molinder, R., Weiland, F., Wiinikka, H., Öhman, M., Öhrman, O.G. W., 2014. Slag formation during oxygen-blown entrained-flow gasification of stem wood. *Energy Fuels* 28, 6941–6952. <http://dx.doi.org/10.1021/ef501496q>.
- [28] Perander, M., DeMartini, N., Brink, A., Kramb, J., Karlström, O., Hemming, J., Moilanen, A., Konttinen, J., Hupa, M., 2015. Catalytic effect of Ca and K on CO₂ gasification of spruce wood char. *Fuel* 150, 464–472. <http://dx.doi.org/10.1016/j.fuel.2015.02.062>.
- [29] Kirtania, K., Axelsson, J., Matsakas, L., Christakopoulos, P., Umeki, K., Furusjö, E., 2016a. Kinetic study of catalytic gasification of wood char

BIBLIOGRAPHY

- impregnated with different alkali salts. *Energy* 1–11. <http://dx.doi.org/10.1016/j.energy.2016.10.134>.
- [30] Song, W., Tang, L., Zhu, X., Wu, Y., Rong, Y., Zhu, Z., Koyama, S., 2009. Fusibility and flow properties of coal ash and slag. *Fuel* 88, 297–304. <http://dx.doi.org/10.1016/j.fuel.2008.09.015>.
- [31] Bell D, Towler B, FanM. Coal gasification and its applications [Internet]. Available from: https://books.google.com/books?hl=en&lr=&id=UZNtdSGt64EC&oi=fnd&pg=PP2&dq=Coal+gasification+and+its+applications&ots=dDyYiDDsPp&sig=fn90_srARxVShIF6P-Kv_iYOGVw.
- [32] R. Radmanesh, J. Chaouki, C. Guy, *AIChE J.* 2006, 52, 4258.
- [33] Vassilev SV, Baxter D, Andersen LK, et al. An overview of the chemical composition of biomass. *Fuel* [Internet]. 2010;89(5):913–933. Available from: <https://doi.org/10.1016/j.fuel.2009.10.022>.
- [34] Majid Emami-Meibodi & MohammadReza Elahifard (2017): A Gibbs energy minimization study on the biomass gasification process for methanol synthesis, *Biofuels*, DOI:10.1080/17597269.2017.1358942 <http://dx.doi.org/10.1080/17597269.2017.1358942>
- [35] Optimal Integrated Plant for Production of Biodiesel from Waste. Borja Hernández and Mariano Martín. *ACS Sustainable Chemistry & Engineering* 2017 5 (8), 6756-6767. DOI: 10.1021/acssuschemeng.7b01007
- [36] Hernandez, B.; Martín, M. Optimal Process Operation for Biogas Reforming to Methanol: Effects of Dry Reforming and Biogas Composition. *Ind. Eng. Chem. Res.* 2016, 55, 6677–6685.
- [37] K. Aasberg-Petersen, C. Stub Nielsen, I. Dybkjær, J. Perregaard, Large Scale Methanol Production from Natural Gas, Haldor Topsøe Brochure. URL: http://www.topsoe.com/business_areas/methanol/~media/PDF%20files/Methanol/Topsoe_large_scale_methanol_prod_paper.ashx (last accessed 4.04.13).
- [38] J. Ott, V. Gronemann, F. Pontzen, E. Fiedler, G. Grossmann, D. B. Kersebohm, G. Weiss, and C. Witte, Methanol, in *Ullmann's Encyclopedia of Industrial Chemistry* (Wiley-VCH Verlag GmbH & Co. KGaA, Weinheim, Germany, 2012).
- [39] I. Wender, Reactions of synthesis, *Fuel Processing Technology* 48, 189 (1996).
- [40] E. Fiedler, G. Grossmann, D.B. Kersebohm, G. Weiss, C. Witte, Methanol, in: *Ullmann's Encyclopedia of Industrial Chemistry*, 6th ed., Wiley-VCH GmbH, Weinheim, 2003, p. 611.
- [41] V. Gronemann, L. Plass, and F. Schmidt, Commercial Methanol Synthesis from Syngas, in *Methanol: The Basic Chemical and Energy Feedstock of the Future*, edited by M. Bertau, H. Offermanns, L. Plass, F. Schmidt, and H.-J. Wernicke (Springer, 2014) Chap. 4.7, pp. 234–266.
- [42] Mathematical modeling of internal mass transport limitations in methanol synthesis B.J.Lommerts, G.H.Graaf, C.M.Beenackers, [https://doi.org/10.1016/S0009-2509\(00\)00194-9](https://doi.org/10.1016/S0009-2509(00)00194-9)
- [43] G.H. Graaf, H. Scholtens, E.J. Stamhuis, A.A.C.M. Beenackers, *Chemical Engineering Science* 45 (1990) 773–783.

BIBLIOGRAPHY

- [44] G.H. Graaf, P.J.J.M. Sijtsema, E.J. Stamhuis, G.E.H. Joosten, *Chemical Engineering Science* 41 (1986) 2883–2890.
- [45] KINETICS OF LOW-PRESSURE METHANOL SYNTHESIS G. H. GRAAF, E. J. STAMHUIS, A. A. C. M. BEENACKERSZ Department of Chemical Engineering, State University of Groningen, Nijenborgh 1&9747 AC Groningen, Netherlands
- [46] Simulation and optimization of a methanol synthesis process from different biogas sources, Rafael Oliveira dosSantosLizandro de SousaSantosDiego MartinezPrata, <https://doi.org/10.1016/j.jclepro.2018.03.108>
- [47] Effect of operating parameters on methanation reaction for the production of synthetic natural gas
Korean Journal of Chemical Engineering, 2013, Volume 30, Number 7, Page 1386
Woo Ram Kang, Ki Bong Lee
- [48] Novel efficient process for methanol synthesis by CO₂ hydrogenation
Anton A. Kiss, J.J. Pragt, H.J. Vos, G. Bargeman, M.T. de Groot
- [49] Kauw, M. (2012). Recycling of CO₂, the perfect biofuel? *Default journal*.
- [50] E. Supp, R.F. Quinkler R.A. Meyers (Ed.), *The Lurgi low-pressure methanol process. Handbook of synfuels technology*, McGraw-Hill (1984), pp. 113-131
- [51] Lurgi MegaMethanol, <https://www.engineering-airliquide.com/lurgi-megamethanol>
- [52] Lurgi <http://www.zeogas.com/files/83939793.pdf>
- [53] METHANOL AND DERIVATIVES PROVEN TECHNOLOGIES FOR OPTIMAL PRODUCTION, *Air liquid engineering and construction*
- [54] Efficient methanol synthesis: Perspectives, technologies and optimization strategies, GiuliaBozzano,FlavioManenti, <https://doi.org/10.1016/j.pecs.2016.06.001>
- [55] Optimization of Inlet Temperature of Methanol Synthesis Reactor of LURGI Type, BenjamínCañete,Nélida B.Brignole,Carlos E.Gigola
DOI: 10.4028/www.scientific.net/AMR.443-444.671
- [56] Lurgi's Mega-Methanol technology opens the door for a new era in down-stream applications, JürgenHaid,UlrichKoss, [https://doi.org/10.1016/S0167-2991\(01\)80336-0](https://doi.org/10.1016/S0167-2991(01)80336-0)
- [57] Lurgi MegaMethanol Technology – Delivering the building blocks for future fuel and monomer demand, Presented at the DGMK Conference “Synthesis Gas Chemistry“,October,4.–6.,2006,Dr.Thomas Wurzel, Lurgi AG, https://www.dgmk.de/petrochemistry/abstracts_content14/Wurzel.pdf

BIBLIOGRAPHY

Ringraziamenti

Vorrei ringraziare il prof. Visconti, relatore di questa tesi di laurea, oltre che per l'aiuto fornitomi in questo anno di lavoro e per la conoscenza passatami durante gli incontri effettuati, per la precisione e la metodologia che mi ha trasmesso e che mi sono stati di esempio per questo elaborato e lo saranno per i successivi.

Un grande ringraziamento va a mia madre Ada e mio padre Rodolfo, i perni della mia vita. Da loro ho imparato tutto ciò che di buono ho in me. La perseveranza e la tenacia che mi hanno insegnato è stata la fonte principale dei miei successi, avvenuti solo grazie ai loro sacrifici. Sin da quando ero piccolo mi hanno insegnato a non mollare mai e puntare in alto. Vederli sorridere oggi per questo mio traguardo mi fa sentire soddisfatto, perché ho sempre creduto che il giusto ringraziamento a quello che loro fanno per me, sia donare risultati che li rendono felici. Vederli orgogliosi di quello che sono diventato mi spinge a continuare in quello che sto facendo ed a migliorare. Da non sottovalutare poi, il contributo economico che mi ha permesso di completare il mio corso di studi. Sarà mia premura far vedere loro che il loro sostegno complessivo è stato sfruttato al meglio e sarà mia premura ripararli nel miglior modo possano volere. Vi voglio bene!

Vorrei inoltre ringraziare i miei fratelli Egidio e Giulia. Con entrambi ho percorso questo cammino ed entrambi conoscono le fatiche che posso aver incontrato per completarlo.

Ricordo ancora quando, il primo giorno arrivato a Milano, in casa con Egidio, mi disse una frase che non ho mai dimenticato: "Domè, se studi per prendere 18, verrai bocciato, se studi per prendere 30, prenderai sicuramente meno". Beh, questa frase mi è rimasta impressa in mente ed è stato il mio "mantra" durante gli anni universitari. Non ho mai studiato per un voto, ma solamente per soddisfare la mia voglia di sapere. Un grazie a lui perché si è rivelato la guida necessaria al compimento di questo viaggio. I suoi consigli preziosi, che molto spesso si concludevano con un "sei un minchione", sono stati sempre ascoltati con gli occhi di un fratellino che pendeva dalle parole del suo fratellone.

E ricordo anche la filosofia di Giulia. Più sbarazzina e meno autoritaria di Egidio, ad ogni esame mi diceva: "Dumè accetta e laureati, non stare a guardare il voto se le cose le sai bene". Beh, questa filosofia per alcuni versi è complementare a quella detta prima. Un grazie a lei perché si è presa cura di me nei momenti difficili (vedersi la sua bellissima "vacanza" a Stoccolma, ti è piaciuto il tour degli ospedali?), mi ha sollevato il morale quando ero giù e cucinava sempre tante cose buone per soddisfare il mio palato (sì, come nò e chi ci crede). È stata sempre, come gli altri 3 membri, il modello a cui mi sono basato. Sempre lì pronta a scherzare con me, a farmi sorridere ed arrabbiare (la maggior parte delle volte).

Ringrazio i miei parenti. Nonostante oggi non ci siano, sono sempre stati presenti nella mia vita. Dalla “banana” di nonna Assunta, ai video e le battute di zia Rosanna, agli scherzi con Zio Pio e Zia Rosalia ed a tutti gli altri, io dico grazie. Avete contribuito costantemente a rendere questo percorso più semplice. Avete portato gioia e felicità in me. Se non oggi, avrò l’occasione di ringraziarvi di persona e di rendervi partecipi di questo risultato finale.

Vorrei ringraziare inoltre i miei amici, i presenti e i non, i “Milanesi” ed i Materani. Se sono quel che sono lo devo anche a loro. Dalla miscela di cultura, comportamenti e caratteri, mi sono plasmato. Grazie per aver condiviso con me i vostri momenti e le vostre esperienze. Tra le cene a tema, le serate in discoteca, le birre, le partite a carte, i “vinelli e scopa”, i giri tra i Sassi, i giochi da tavola, le litigate su monopoli (eddai, lasciatemi comprare settecento cassette), le fantasie su Dixit etc etc. Ne potrei dire altre mille ma non sto qui a dilungarmi. Grazie per tutte le risate, per tutte chiacchierate e per i caffè. Ognuno di voi merita un ringraziamento speciale perché davvero tutto questo è stato più bello con voi.

Vorrei ringraziare Luciana e la sua famiglia. Tutte le cene insieme, i momenti di imbarazzo costantemente seguiti da quelle burlone così simpatiche che prendevano in giro, le sere passate in vostra compagnia, le giornate al mare, sono state momento essenziale che mi ha sempre aiutato a sgomberare la mente dai problemi dell’università. Grazie di avermi supportato (o dovrei dire sopportato), di avermi incoraggiato e di avermi sempre fatto sentire parte della famiglia rendendo il tutto più facile.

Apro una parentesi per lei. Dovrei ringraziarti per tante cose a questo punto. Mi hai sopportato (e questa volta non sbaglio) durante tutti i momenti difficili. Hai ascoltato praticamente tutti gli esami che ho fatto nel mio percorso (infatti avevo sentito volessero proclamare anche te). Sei stata costantemente quella persona che mi ha fatto vedere il mondo da un secondo punto di vista, non sempre giusto, ma che mi ha aiutato a comprendere come meglio avrei potuto procedere. Ad ogni mio traguardo, positivo o negativo, eri lì a dirmi: “bravo Dò, sono fiera di te”. Ogni mio giorno prima dell’esame eri lì a dirmi: “tranquillo, andrà tutto bene, lo sappiamo che sei bravo (mi dicevi anche RILEGGI)”. La tua filosofia di vita, di cui ne vado fiero e di cui ne condivido gran parte, è sempre stata piena di positività, tenacia e voglia di fare. Ti ringrazio perché sei stata un perno per me, un’ancora di salvezza a cui aggrapparmi, sempre con la sicurezza che mi avresti sostenuto in ogni mia peripezia. Se sono la persona che sono ora, lo devo anche grazie a te, che in 7 anni sei riuscita a cambiarmi, migliorarmi e maturarmi. Mi hai reso un uomo migliore.

A tutti voi io dico grazie e dedico questa laurea. Vedervi felici e fieri di me, è il traguardo più importante potessi raggiungere.

